Substrate curvature as a cue to guide spatiotemporal cell and tissue organization

Callens, Sebastien J.P.; Uyttendaele, Rafael J.C.; Fratila-Apachitei, Lidy E.; Zadpoor, Amir A.

DOI
10.1016/j.biomaterials.2019.119739

Publication date
2020

Document Version
Final published version

Published in
Biomaterials

Biomaterials 232 (2020) 119739

Contents lists available at ScienceDirect

Biomaterials

journal homepage: www.elsevier.com/locate/biomaterials

Review

Substrate curvature as a cue to guide spatiotemporal cell and tissue organization

Sebastien J.P. Callens*, Rafael J.C. Uyttendaele, Lidy E. Fratila-Apachitei, Amir A. Zadpoor

Department of Biomechanical Engineering, Delft University of Technology (TU Delft), Mekelweg 2, Delft, 2628CD, the Netherlands

A B S T R A C T

Recent evidence clearly shows that cells respond to various physical cues in their environments, guiding many cellular processes and tissue morphogenesis, pathology, and repair. One aspect that is gaining significant traction is the role of local geometry as an extracellular cue. Elucidating how geometry affects cell and tissue behavior is, indeed, crucial to design artificial scaffolds and understand tissue growth and remodeling. Perhaps the most fundamental descriptor of local geometry is surface curvature, and a growing body of evidence confirms that surface curvature affects the spatiotemporal organization of cells and tissues. While well-defined in differential geometry, curvature remains somewhat ambiguously treated in biological studies. Here, we provide a more formal curvature framework, based on the notions of mean and Gaussian curvature, and summarize the available evidence on curvature guidance at the cell and tissue levels. We discuss the involved mechanisms, highlighting the interplay between tensile forces and substrate curvature that forms the foundation of curvature guidance. Moreover, we show that relatively simple computational models, based on some application of curvature flow, are able to capture experimental tissue growth remarkably well. Since curvature guidance principles could be leveraged for tissue regeneration, the implications for geometrical scaffold design are also discussed. Finally, perspectives on future research opportunities are provided.

1. Introduction

Complex shapes are omnipresent in our physical world and are found at all length scales, ranging from nanostructured materials [1] to the abstract shape of the universe [2]. Such shape complexity is also observed in biology, and the intriguing way it could emerge from a single zygote forms a central topic in embryogenesis. It has long been understood that biological form and function are intimately connected, and that mechanical forces are at play in the growth of complex biological shapes [3]. The appreciation for this interplay between force and shape on one hand, and biology on the other, has laid the foundation for mechanobiology as an important discipline explaining cell behavior [4]. Indeed, it is now well established that the physical aspects of a cell's surroundings deserve as much attention as the chemical nature of the environment. For example, cell shape, motility, and fate could all be affected by physical cues in the environment such as stiffness [5,6], viscoelasticity [7], or the applied mechanical stretch [8,9]. These physical cues are sensed by cells through integrin-mediated force-feedback between the cell and the extracellular matrix (ECM) or through cell-cell interactions, and elicit a cell-level response that contributes to the emergent organization of tissue and organism shapes [10–12]. The transduction of physical signals into biochemical responses is enabled through mechanotransduction pathways, which are not limited to conformation-dependent molecular processes at the cell surface but also involve the nucleus, being mechanically linked to the ECM through the cytoskeleton [10,13].

In addition to material-dependent physical cues [14], purely shape-dependent signals can also affect cell response. For example, it has long been known that small-scale topographies in the environment (*e.g.*, grooves or pillars) could affect cell fate and motility [15–18]. In addition to such sub-cellular-scale features, however, it is now understood that the three-dimensional (3D) shape of the environment at a larger scale ($\geq$ cell size) can also guide cell and tissue behavior [19]. As such, it is of crucial importance to be able to quantitatively describe the (3D) shape of the cell environment. This may be best achieved using the notion of surface curvature. Surface curvature is a fundamental concept within the mathematical field of differential geometry, capable of describing the local geometry of a 3D object (*i.e.*, the geometry of the bounding surface of that object). Indeed, a rapidly growing body of experimental evidence, supported by computational insights, shows that the organization, dynamics, and fate of individual cells can be influenced by substrate curvature, on a scale larger than the individual cell size. Furthermore, the impact of substrate curvature extends to the tissue level, and affects both the temporal and spatial organization of tissue growth.

Here, we review the recent evidence demonstrating the role of substrate curvature on cell organization and motility, as well as on *de novo* tissue growth. We first introduce the “language of shape” [20] in

* Corresponding author.
E-mail address: s.j.p.callens@tudelft.nl (S.J.P. Callens).

https://doi.org/10.1016/j.biomaterials.2019.119739
Received 18 September 2019; Received in revised form 23 December 2019; Accepted 25 December 2019
Available online 27 December 2019

terms of the formal descriptions of surface curvature, aiming to provide a bridge between the fields of differential geometry and biology. Then, we discuss the response of individual cells to mesoscale substrate curvature and address the specific roles of intracellular components, such as the cytoskeleton and the nucleus. Next, we move on to the collective behavior of cells, starting with cell monolayers and continuing with more advanced (often bone-like) tissue constructs. We also show how cell and tissue-level computational models can reproduce many of the experimental observations on curvature guidance. Understanding the response of cells and tissues to substrate curvature is important, not only to elucidate the mechanisms involved in tissue morphogenesis, pathology, and repair, but also to advance the development of novel biomaterial strategies for tissue engineering and regenerative medicine. Therefore, we also briefly address the implications of the reviewed curvature guidance principles for scaffold design. We conclude with an outlook on future research directions.

2. Understanding substrate curvature

2.1. A geometrical treatment of curvature

The concept of curvature is unavoidable to everyone attempting to describe shape. Whether dealing with lines, surfaces, or higher-dimensional objects, curvature is a fundamental geometrical property that provides *local* information about the shape of the object. Though intuitive to some extent, curvature is often informally treated in applied contexts using ambiguous terms such as “concavity” and “convexity” that do not capture its full complexity. However, the field of differential geometry provides formal curvature definitions, enabling precise and unambiguous descriptions of the *local* shape of objects. Here, we aim to introduce these definitions and equip the reader with a more formal understanding of surface curvature, in order to better discuss its relevance within mechanobiology.

Perhaps the most intuitive notion of curvature is that of a curved line drawn on a two-dimensional plane. In this case, the curvature can be calculated at any point along the line as the reciprocal of the radius of the osculating circle at that point (Fig. 1a). The curvature of this one-dimensional (1D) line embedded in a two-dimensional (2D) plane provides a measure for how much the line deviates from a straight line at any particular point. Increasing the dimension by one order, it is possible to consider the curvature of a two-dimensional (2D) surface that is embedded in three-dimensional (3D) space. Analogous to the previous case, the surface curvature is again evaluated at a single point, and it describes how the surface deviates from the tangent plane at that point [21]. This means that curvature is a *local* property of a surface. It is, therefore, not possible to assign a single value of curvature to a surface, unless that surface has constant curvature. Within the context of this paper, we are concerned with this concept of surface curvature. That is, we are interested in the curvature of the outer surface of the substrates that cells are situated on. Surface curvature is an inherently more complex concept than the curvature of a line in a 2D plane, since surface curvature depends on the direction that is being considered. For example, a surface might be curved in one direction while remaining flat in the orthogonal direction (*e.g.*, the curvature of a cylinder). To quantitatively describe surface curvature, two important measures have been established, namely the *mean curvature,* H, and the *Gaussian curvature,* K, both of which are useful and provide complementary perspectives on curvature.

To define both mean and Gaussian curvatures, it is useful to first introduce the *principal curvatures* at a point on the surface. Imagine intersecting a curved surface at a given point with a normal plane, *i.e.* a plane that contains the normal to the surface at that point. The plane and the surface intersect along a curved line, with normal curvature κ_n (determined as the inverse of the radius of the osculating circle, $\kappa_n = 1/r_n$). Rotating through all possible normal planes at this particular point yields a maximum and minimum value for the normal curvature, which are the principal curvatures, κ_1 and κ_2, of the surface at that point. The principal curvatures can then be used to define both the mean (H) and Gaussian (K) curvatures as:

$$H = \frac{1}{2}(\kappa_1 + \kappa_2) \tag{1}$$

$$K = \kappa_1 \cdot \kappa_2 \tag{2}$$

For every point on a curved surface, it is possible to calculate a single real-valued mean and Gaussian curvature using the above definitions. Note that both measures are dimensional, with the mean curvature having the dimension $[1/l]$ and the Gaussian curvature having the dimension $[1/l^2]$, where l is the length dimension. A flat plane, not surprisingly, has mean and Gaussian curvatures of zero, since $\kappa_1 = \kappa_2 = 0$. Rolling a flat plane into a cylinder produces nonzero mean curvature, but leaves the Gaussian curvature unaffected since one of the two principal curvatures remains zero for a cylinder. To achieve nonzero Gaussian curvature, both principal curvatures have to be nonzero. This is, for example, the case on a sphere, where the principal curvatures are equal and positive, or on a saddle, where the principal curvatures have opposite sign (Fig. 1a). As a consequence, the Gaussian curvature is always positive on sphere-like or “elliptic” geometries ($K > 0$) while it is negative for saddle-like or “hyperbolic” geometries ($K < 0$). It is important to realize that the sign of the Gaussian curvature is an important indicator of the type of surface that is dealt with, since it remains unchanged regardless of the side of the surface being considered. For example, the Gaussian curvature of a point on a sphere is always positive, no matter when looking at the outside (“convex” part) or inside (“concave” part) of the sphere. This is different for the sign of the mean curvature, which depends on the chosen convention for the positive and negative principal curvatures, *i.e.* it depends on the chosen direction of the surface normal. This fact hints at a deeper difference between the mean and Gaussian curvatures: the mean curvature is an extrinsic measure, meaning that it can be defined from outside the surface, while the Gaussian curvature is an intrinsic measure, which can be defined from *within* the surface itself [20–22]. Otherwise stated, a resident living on a curved surface would be able to measure the Gaussian (or the intrinsic) curvature of that surface. This could, for example, be achieved by calculating the sum of the interior angles of a triangle drawn on the surface. On an intrinsically flat surface, such as a plane or a cylinder, the sum of the interior angles would equal π. On a spherical surface, however, the sum of the interior angles would exceed π, while the sum would be less than π on a saddle-shaped surface. It would, therefore, be possible to extract information about the intrinsic curvature of the surface merely by measuring the angles within a surface. This is, however, not true for the mean or extrinsic curvature, as this type of curvature depends on the way the surface is embedded in the reference 3D space. That is, the resident living on the surface would not be able to distinguish between, say, a cylinder and a flat plane [21].

While surface curvature remains a local property, an intimate relationship between the curvature of a surface and its global topology, or “connectedness”, exists. The Gauss-Bonnet theorem dictates that the area-integrated Gaussian curvature, or the total curvature of a surface is proportional to the genus (g) of that surface, which is a topological invariant describing the number of “handles” of the surface [20]:

$$\int_A K da = 4\pi(1 - g) \tag{3}$$

The Gauss-Bonnet theorem, therefore, shows that any surface with given genus, g, has the same integral Gaussian curvature. Moreover, the genus provides information on the sign of the integral Gaussian curvature. A surface with g= 0 (*e.g.*, a sphere), should have a positive integral Gaussian curvature. A surface with g= 1 (*e.g.*, a torus), has zero integral Gaussian curvature. Indeed, the region with positive Gaussian curvature on the outside of the torus is balanced by the negative Gaussian curvature on the inside. Any surface with a higher genus, has

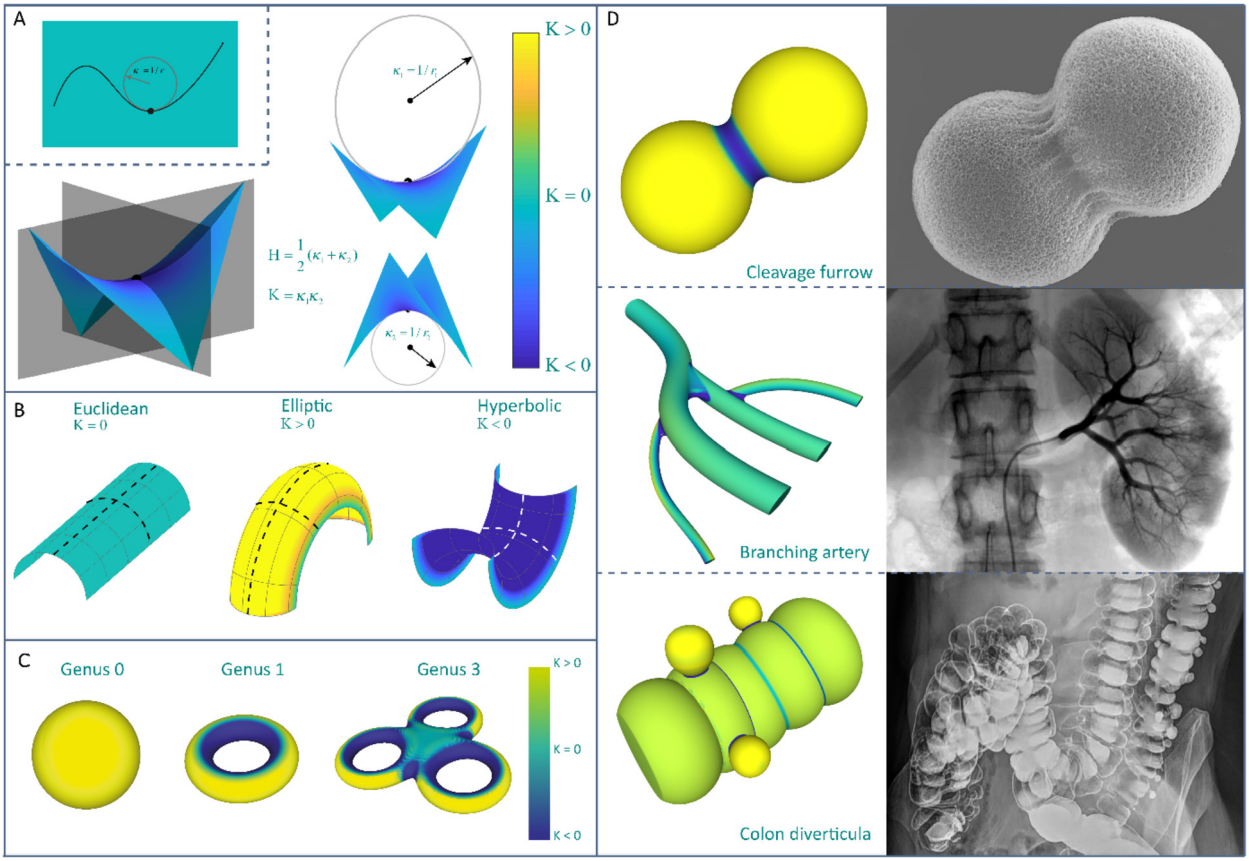

Fig. 1. The definition of surface curvature and some examples from biology. a) Top left inset displays curvature of a 1D line embedded in a 2D plane. Remainder of the panel displays mean (H) and Gaussian (K) surface curvatures as functions of the principal curvatures, demonstrated on a saddle shape. b) Some examples of intrinsically flat and intrinsically curved geometries: a cylinder (left), an elliptic surface (middle), and a hyperbolic surface (right). c) The relation between the genus of a surface (topology) and the Gaussian curvature of that surface. d) Some examples of Gaussian curvature in biological structures. Top: a cleavage furrow during cytokinesis [211]. Middle: Branching in an arterial network [212]. Bottom: Diverticula on the colon [213].

negative integral Gaussian curvature (Fig. 1c). In other words, surfaces with g>1 are, in an integral sense, hyperbolic [20].

Equipped with these definitions of the mean and Gaussian curvatures, it is possible to more formally describe the surface curvature and link it to the mechanobiological response of cells. It should be clear that surface curvature should primarily be discussed using these formal descriptors, and not solely using ambiguous terms such as “convex” and “concave” surfaces. For example, the inner surface of a cylinder and a spherical cap could both be considered as concave, but they are very different from a more formal curvature perspective (*i.e.*, a cylinder has $K = 0$ everywhere whereas a sphere has $K > 0$ everywhere). Moreover, the inner and outer sides of a sphere surface are often distinguished from each other using convexity and concavity, but could more formally be described using mean and Gaussian curvatures: the Gaussian curvature is the same for both cases (and it is positive), but the mean curvatures are opposite in sign. The usefulness of convexity and concavity fades further away when discussing saddle surfaces ($K < 0$), which are convex in one direction and concave in another. Hence, the usage of the terms “convex” and “concave” should be accompanied by the more formal descriptions of the mean and Gaussian curvatures.

2.2. Examples of curved biological shapes

While *in vitro* biological experiments often deal with cells that are constrained to 2D flat surfaces, the natural environment that cells inhabit *in vivo* is 3D, and can be highly complex. The extracellular environment is not only complex due to its hierarchical and composite nature, but is also structured in such a way that gives rise to spatially varying Gaussian and mean curvature distributions, resulting in a myriad of shapes that are geometrically and topologically more complex than planar surfaces. Curvature appears on various scales in biological matter, ranging from the sub-cellular (radius of curvature $\approx 10^1 - 10^3\, nm$) to the supra-cellular scales (radius of curvature $\approx 10^1 - 10^3\, \mu m$), and plays an important role in both morphogenesis and pathology [23,24]. On the smallest scale, lipid bilayer membranes can take on complex curved shapes, a consequence of the interplay between the biochemistry of the membrane formation, membrane mechanics, and geometrical frustration [25–27]. Examples of intrinsically curved membrane structures are membrane-bound spherical vesicles (positive Gaussian curvature), cleavage furrows during cytokinesis (negative Gaussian curvature) [26], or the intracellular structures of the endoplasmatic reticulum and the Golgi apparatus [25] that exhibit high degrees of curvature variation. More convoluted membrane organizations have also been observed, whereby the membrane adopts a 3D minimal surface morphology with cubic periodicity, for example, in the mitochondria of giant amoebae *Chaos carolinensis* [28,29]. It is, however, the curvature that appears on a larger scale in the extracellular environment that we are primarily concerned with in this paper. A high level of shape complexity is observed throughout many organs, which are lined by epithelial tissue. One type of recurring geometry that is, to some extent, representative for many epithelial tissue constructs are cylindrical structures. Examples are tubular vessels, ranging from small capillaries to large arteries, tubular glands, and ducts [30]. Despite their tubular nature, the geometry of these biological structures quickly deviates from mathematically defined cylinders (with zero Gaussian curvature everywhere) once the tubular structures

are bent or branched, as this introduces curvature in the second principal direction, hence resulting in regions with positive or negative Gaussian curvatures (Fig. 1d). The intricate epithelial geometries of complex organs, such as the kidney, lung or intestine, all emerge from a simple planar cell sheet during embryonic development [31]. Interestingly, this morphogenetic sculpting from a planar to a complex, curved geometry is not solely driven by genetic factors, but also relies heavily on thin-sheet mechanics. It has been found that mechanical instabilities in cell sheets, in the form of buckling and wrinkling, could drive the morphogenesis of the cerebral cortex [32], intestinal villi [33], airway branching [34], or tooth development [31,35]. Such mechanical instabilities arise as a consequence of a faster growth of the epithelial sheet with respect to the constraining mesenchyme that surrounds it, causing the sheet to buckle within the mesenchyme (in engineering mechanics, this problem is known as the buckling of a plate on an elastic foundation [36]). The mechanical forces applied to flat epithelia could, therefore, explain much of the spontaneous formation of complex curvature distributions during morphogenesis. The convoluted geometries that arise from these instabilities could, in turn, control further morphogenesis, for example, by regulating the spatial patterns of cell proliferation [37,38] or by controlling the spatial distribution of morphogens [23]. In addition to epithelial morphogenesis, complex curvatures could also emerge during disease, for example, in colonic diverticulosis [39] or polycystic kidney disease [40]. In both cases, outwards-bulging spherical pouches are formed on the colon (Fig. 1d) or kidney respectively, characterized by a primarily positive Gaussian curvature, with negative Gaussian curvature in the neck region. Some similar types of curvature distributions could be observed in the presence of tumors. In fact, tumorigenesis has been found to be partly controlled by geometrical cues, such as curvature [24,41]. In mice pancreatic ducts subject to oncogenic transformation, for example, the direction of tumor growth was found to depend on the radius of curvature of the duct: tumors expanded outwards on narrow ducts (exophytic), while they grew inwards on larger ducts (endophytic) [24].

Among the other types of tissue, osseous tissue is also well known to exhibit complex curvature fields. At a small scale, osteoclasts generate small pits and trenches in the surface of the mineralized matrix during bone resorption, resulting in local curvature variations sensible by osteocytes and osteoblasts. On a slightly larger scale, however, bone tissue is also characterized by complex curvature distributions, particularly trabecular bone. The network-like structure of trabecular bone has been shown to be characterized by an average negative Gaussian surface curvature, rendering trabecular bone on average “hyperbolic” or saddle-shaped [42,43]. Moreover, the average mean surface curvature of trabecular bone was found to be close to zero ($H \approx 0$), attributed to an energy-minimizing bone formation process [42].

It should be clear that a plethora of curved biological structures exists, and that truly flat structures are rather the exception than the rule in native tissues. However, the question of scale should not be neglected when discussing curvature, as this only makes sense when doing so relative to the cell size. For example, very low values of curvature, with very large radii of curvature, might not be “noticed” by the cells at all. On the other hand, very high values of curvature, with radii much smaller than the characteristic cell length, should be considered more as a topographical feature (*i.e.* micro- or nanotopographies [15,17,44,45]) rather than a truly curved substrate. At such small scales, curvature is manifested in the form of local, curved deformations in the cell membrane [10]. In this case, BAR (Bin/Amphiphysin/Rvs) domain proteins have been known to be involved, both as curvature generators and as curvature sensors [46]. Due to the inherent curved nature of these BAR domains, they could impose curvature in initially flat membranes when binding to the membrane through electrostatic interactions [47]. Alternatively, the BAR domain structures could act as sensors of already curved membranes (*e.g.,* curved due to an external geometrical feature) by preferentially binding to these curved portions of the membrane and recruiting small G proteins [10,48]. Because the cell membrane is a bilayer, curving it will induce differences in stress distributions between both sides of the membrane, which could lead to ion channel opening in the membrane [49]. It has been suggested that this selective channel opening could constitute another curvature sensing mechanism [10]. While membrane curvature is important for various cell processes, such as endocytosis [50] and membrane fusion [51], we are dealing with curvature at much larger length scales in this paper, and we refer the interested reader to other reviews on the physics behind membrane curving [46,47,51]. For the remainder of this review, we will focus on substrate curvature on length scales equal to or higher than that of typical (mammalian) cell sizes, *i.e.* the radii of curvature in the approximate range of $10^1 - 10^3$ μm.

3. Single cell response to substrate curvature

The appreciation for substrate curvature as a mechanism to guide cellular behavior (*i.e.,* “curvotaxis” [52]) is much more recent than that for other environmental cues such as chemical gradients (“chemotaxis”) or substrate stiffness (“durotaxis”). Nevertheless, there is a growing body of experimental evidence demonstrating that individual cells can respond to substrate curvature in various ways, ranging from initial migratory patterns to the differentiation behavior. While substrate curvature originally seemed to be considered within the perspective of contact guidance, *i.e.* the guiding principle where cells align along (small) ECM fibers [53,54], it is now typically being considered as separate guiding mechanism, *i.e.* “curvotaxis” [52] or “curvature guidance”, rather than a subset of contact guidance [55]. This is primarily due to the larger curvature radii in the context of curvature guidance (≥ cell size) as opposed to the subcellular-scale features in the case of contact guidance.

Despite a rapidly growing interest in single-cell experiments on curved substrates, only a few types of curved geometries have been considered so far, in part due to the challenge of fabricating precisely-defined microscale substrates with controllable curvatures [56]. In many studies, cylindrical substrates have been employed, either by seeding cells on thick (compared to cell size) fibers [54,57–60], or on hemi-cylindrical patterned substrates [61–63]. In addition to these discrete cylindrical geometries, smoothly-varying sinusoidal or “wavy” patterns have also been used [64–66]. From a formal curvature perspective, all these geometries are examples of developable surfaces, which have non-zero mean curvatures ($H > 0$ on the convex parts and $H < 0$ on the concave parts), but zero Gaussian curvature ($K = 0$) everywhere. In addition to cylindrical geometries, substrates patterned with hemispherical convex caps ($H > 0$, $K > 0$) or concave pits ($H < 0$, $K > 0$) have also been employed in several studies [61,67–70], as well as smoothly-varying, wavy patterns of alternating caps and pits [52]. Surprisingly, little research has been performed on the response of cells to substrates with negative Gaussian curvatures ($K < 0$), which are saddle-shaped substrates [30,63]. In this section, we outline recent results on the behavior of individual cells on curved substrates, first by describing how curvature affects cell alignment and migration, and later by addressing the specific roles of cytoskeletal tension and the cell nucleus in sensing and responding to curvature.

3.1. Curvature-guided cell alignment and migration

Cell alignment and migration are the most commonly investigated phenomena in single-cell experiments on curved substrates. Throughout the lifetime of multicellular organisms, cell migration plays a fundamental role in the development, maintenance, pathology, and repair of tissue. Although it is a complicated multi-step process involving bi-directional cell-ECM interactions [71] and variations among different cell types, some basic principles of the cell migration cycle are conserved [72]. An adherent cell migrating on flat surfaces first establishes polarity, developing distinct leading (front) and trailing (rear) edges in the direction of migration. This polarity is characterized by a

polarized cytoskeletal structure and different molecular processes at the front and rear of the cell, regulated in part by Rho GTPases [72–74]. Upon polarization, the leading edge of the cell develops protrusions in the form of broad lamellipodia and "spiky" filopodia, enabled by actin polymerization [72,75]. Subsequently, the protrusions bind to the ECM, forming anchoring points for the cytoskeletal network to exert traction and pull the cell forward over these adhesion sites [73,76]. Finally, detachment at the rear of the cell and the retraction of the trailing edge occurs in order for the cell to translocate across the substrate.

Associated with migration is the tendency of cells to align (and elongate) in response to curvature. Fibroblasts, smooth muscle cells, and mesenchymal stromal cells seeded on cylindrical substrates (convex side, *i.e.*, $H > 0$ and $K = 0$) have been shown to preferentially align their elongated bodies and cytoskeletal structure along the cylinder axis [54,57,61,63–65,77–79]. As such, the cells tend to avoid curvature by aligning along the (principal) direction of zero curvature. Epithelial cells on the other hand, have been found to orient their cytoskeletal structure in circumferential direction and "wrap" the cylindrical substrate [58–60,80], thereby aligning in the (principal) direction of maximum curvature. In experiments with fibroblasts on cylindrical substrates, the degree of longitudinal alignment was found to increase with curvature (*i.e.*, a decreasing radius of curvature) [57,61,63]. Indeed, the scale of the substrate curvature is important, since too large curvature radii (*i.e.*, $\kappa \gg$ cell size) cannot be detected by individual cells. Interestingly, sufficiently large curvature cues could overrule a competing cue in the form of nanoscale contact guidance in determining cell alignment [61]. While cylinders could induce preferential cell alignment, this is not observed on spherical substrates ($K > 0$), because the curvature is constant in all directions (both the mean and Gaussian curvatures are constant and positive on a sphere). As opposed to cylinders, there is no option for cells on spheres to find an orientation that either minimizes or maximizes curvature. In this regard, it would be interesting to observe cellular alignment on ellipsoidal substrates ($K > 0$ and varying), where the principal curvature in one direction is higher than in the other. It might be expected that cells with pronounced stress fibers would then align preferentially along the direction with the lowest curvature. Furthermore, cell alignment on saddle surfaces ($K < 0$) is still largely unexplored [30,63].

In addition to static cell body alignment, time-lapse microscopy has revealed that substrate curvature also impacts directional cell migration. Human bone-marrow derived stromal cells (hBMSCs) cultured on convex cylindrical substrates ($K = 0$, $H > 0$) were shown to migrate increasingly along the cylinder axis for increasing curvatures (decreasing radii) [61,63]. However, hBMSCs on concave cylindrical substrates ($K = 0$, $H < 0$) were shown to exhibit a non-aligned and non-persistent migration mode without angular preference [63]. In the case of T-cells seeded on sinusoidal wavy surfaces ($K = 0$, H is varying), a zigzagging migration mode in the concave grooves of the waves ($H < 0$) was observed [66]. On (hemi-)spherical substrates, a different migration behavior has been observed on the convex ($K > 0$, $H > 0$) sides as opposed to the concave ($K > 0$, $H < 0$) sides of the spheres [69,70]. Fibroblasts and mesenchymal stromal cells (MSCs) migrate significantly faster inside concave pits as compared to convex caps and flat surfaces, with no significant difference between the latter two [69,70]. Moreover, two distinct migration modes have been observed: a typical 2D migration response on the convex caps, but a faster, spider-like "extend-and-pull" movement in the concave pits, whereby the cells first form long body extensions that span over the pits, and consequently retract their cell body towards the attachment sites of the extension [69]. On a smoothly varying "double-sinusoid" landscape (Fig. 2f), exhibiting varying mean and Gaussian curvatures, MSCs and fibroblasts consistently migrate into the valleys ($K > 0$, $H < 0$) and avoid the hills ($K > 0$, $H > 0$) along their trajectory, a response that increases with increasing curvature values (Fig. 3d) [52]. During the migration phase, the nuclei of the cells are first located near the deepest point of the valleys, while the cell protrusions probe the environment.

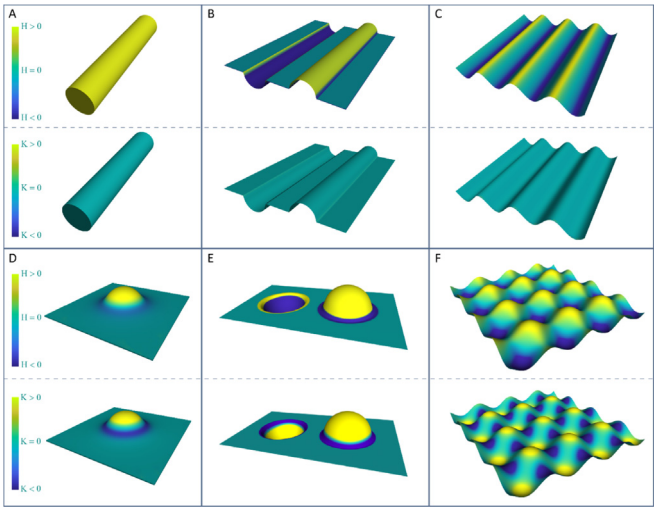

Fig. 2. Some examples of the curved substrates used in single-cell experiments. The mean (top) and Gaussian (bottom) curvature distributions of cylinders (a), hemicylindrical substrates (b), sinusoid wavy substrates (c), sphere-with-skirt substrate (d), hemispherical substrates (e), and double-sinusoid wavy substrate (f). While a-c are examples of developable (intrinsically flat) surfaces, *d*-f showcase non-developable (intrinsically curved) surfaces.

During a translocation step, the nuclei quickly locate from one valley to the next, reaching high velocities on the hills. This increased velocity on the convex parts is conflicting with some of the earlier results [69,70], but is likely a consequence of the dynamic exploration behavior of the cells in this smoothly varying, hilly landscape, as opposed to the more discrete, separated hemispheres in other studies. The observation that cells avoid convex spherical caps ($K > 0$, $H > 0$) is common [30,67,68], provided that the curvature values are sufficiently large (*e.g.*, spheres with $r < 500\,\mu m$ for fibroblasts [67]). In addition to fibroblasts or stromal cells, this observation is also made with macrophages (Fig. 3d bottom): cells avoid the regions with positive values of mean and Gaussian curvatures (*i.e.*, convex caps) and actively migrate into regions of negative mean and positive Gaussian curvatures (*i.e.*, concave pits) [68]. In curvature landscapes with larger feature sizes, however, macrophages do not exhibit this curvature-driven behavior, potentially due to relatively lower curvature values as compared to the macrophage cell size [52]. Despite the general avoidance of convex caps, however, active cell migration on shallow convex caps has been observed in some studies [70,81]. These shallow caps are spherical sections with an aspect ratio below 0.5, which would correspond to a hemispherical section. Such shallow convex caps may pose less of an obstruction to the cells migrating from the flat surroundings, as compared to truly hemispherical caps.

While cell migration on developable ($K = 0$) and spherical ($K > 0$) surfaces has been the subject of several studies, cell behavior on hyperbolic ($K < 0$) surfaces is largely unexplored. In one study, axisymmetric sphere-with-skirt substrates have been used for culturing fibroblasts [30]. The substrates consisted of convex caps ($K > 0$) that smoothly transitioned towards the flat surroundings ($K = 0$) through a saddle-shaped region ($K < 0$) (Fig. 2d). Cells on such substrates avoided the convex spherical part of the substrate, but occasionally "probed" it using short-lived lamellipodia [30]. Instead, the cells showed an azimuthal cell polarity and migrated around the cap on the saddle-shaped region. In another recent study, mesenchymal stromal cells were cultured on a saddle-shaped section of a torus, and preferential migration along the concave direction of the saddle was observed [63]. While deliberate investigations into the response of cells to saddle shapes are still uncommon, it is important to understand that many other substrates also contain saddle-shaped regions. For example, the transition region from a hemispherical cap to the flat surroundings must have a

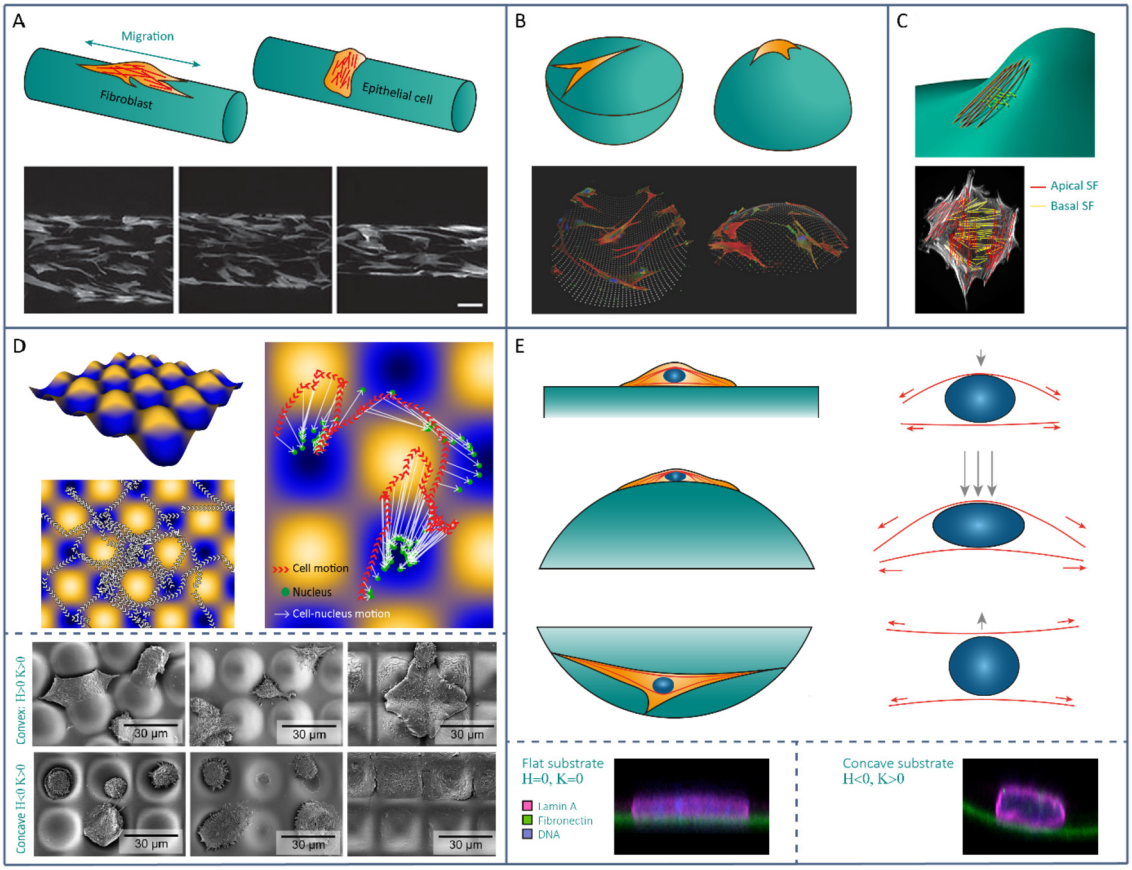

Fig. 3. Single-cell response on curved substrates. a) Fibroblastic-like cells align longitudinally on cylindrical substrates, while epithelial cells wrap the substrates. Insets show increasing hBMSC alignment for increasing curvature on convex cylindrical substrates [61], reproduced with permission from The Royal Society. b) MSCs on concave and convex hemispherical substrates. Insets obtained with permission from Ref. [69] c) Fibroblasts on sphere-with-skirt substrates, exhibiting apical and basal stress fiber alignment, reproduced with permission from Elsevier [30]. d) Top: the migration trajectories of MSCs (obtained with time-lapse microscopy) on double-sinusoid wavy substrates. Obtained with permission from Ref. [52]. Bottom: the positioning of macrophages on substrates with various types of convex hills and concave valleys. Obtained with permission from Ref. [68]. e) Curvature-induced compression of the nucleus on flat, concave spherical and convex spherical substrates. The schematic drawing is adapted from Ref. [69]. Bottom insets show the shape of the nucleus on concave and flat substrates, obtained with permission from Ref. [52].

negative Gaussian curvature, though this region could be very narrow and is typically not considered in curvature-guided cell culture studies (Fig. 2e). Nonetheless, the relevance of hyperbolic geometry in biological tissue necessitates more dedicated investigations to elucidate the role of saddle shapes on cell migration.

3.2. The central role of cytoskeletal mechanics

A recurring theme in the discussions of cell response to curved substrates is the central role that cytoskeletal arrangement and tension seem to play. The contractile stresses that arise in the filamentous cytoskeletal network endow cells with both a sensory function, enabling them to sense the physical properties of their environment [5], and a force generation function [19], not only facilitating cell migration and cytokinesis [82] but also enabling the wrinkling of soft substrates [83] and even cell-scale origami folding [84]. The contraction of the cytoskeleton, which consists of a network of actin microfilaments, intermediate filaments, and microtubules, is governed by the actomyosin machinery, consisting of filamentous actin (F-actin) in conjunction with myosin II motors that sit in between [82]. A crucial ingredient for the contractility-induced sensory and force generating functions is the adhesion of the cells to the substrate that they are situated on and the ability to transmit force [85]. Cells use transmembrane proteins, called integrins, to bind to ligands in the extracellular matrix (*e.g.,* fibronectin). Upon activation by force, several proteins are recruited, such as talin [86] and vinculin [87], through which a mechanical link between the ECM and the actin filaments of the cytoskeleton can be established [88]. Moreover, the exertion of force on the integrins also activates the RhoA signaling pathway, which, through the activation of Rho kinases (ROCK) and myosin light chain (MLC), ultimately triggers the assembly of myosin II filaments [88]. Those myosin II filaments interact with actin to enable contraction and cross-linking [89], and have also been implicated in actin polymerization [90], thereby contributing to the force-induced remodeling of the cytoskeleton, as well as the establishment of mature focal adhesions [88]. In other words, this mechanical interaction between the extracellular environment and the intracellular cytoskeleton results in a force-feedback mechanism that triggers the cell to remodel its cytoskeleton. This force-feedback mechanism will be affected when a cell is situated on a 3D, curved geometry instead of an isotropic planar substrate, which is why cytoskeletal arrangement and contractility are important aspects to consider in any discussion of curvature guidance.

As mentioned before, fibroblasts and MSCs seeded on convex cylindrical substrates ($H > 0,\ K = 0$) typically align longitudinally along the cylinder axis, an effect that increases with curvature. Typically, this global cell alignment is accompanied by an arrangement of stress fibers (*i.e.*, bundles of actin microfilaments) [91] in the longitudinal direction (*i.e.*, in the direction of zero principal curvature) [54,57,61,63,78]. In a seminal work, Dunn and Heath hypothesized that this cytoskeletal arrangement (and cell body alignment) occurs because the stress fibers

cannot assemble or operate in a bent condition (*i.e.*, there is a bending energy penalty), which is why the cells avoid the substrate curvature and align longitudinally [54]. While plausible, this theory does not explain the different behavior exhibited by epithelial cells where stress fibers align circumferentially [58–60]. It has, therefore, been suggested that the cell and cytoskeletal orientation on convex cylindrical substrates ($K = 0,\ H > 0$) is driven by a competition between the bending resistance of the stress fibers and a shear deformation that develops as a consequence of cell contractility [92] (Fig. 6a and Section 5.1). When adhering to a flat substrate, the top surface of the cell is free to contract in the direction of the stress fibers, while the attached (bottom) surface is constrained, resulting in a shear deformation throughout the cell thickness. When the cell is bent along a convex cylindrical substrate, an additional deformation ensues: the top surface is subject to extension while the bottom surface contracts. In this case, it is energetically favorable for the cell to align its stress fibers perpendicularly to the cylinder axis, since the actomyosin-induced contraction could partly compensate for the bending-induced extension. However, this imposes an energetic penalty due to stress fiber bending, which prefer to alignment along the zero-curvature direction [92]. The stress fiber orientation is, therefore, determined by an energy trade-off: longitudinal alignment is predicted when the bending energy dominates (*e.g.*, in the case of thick stress fibers in fibroblasts), while circumferential alignment is predicted when the contractility-term dominates (*e.g.*, for the relatively thin stress fibers in epithelial cells) [92]. Indeed, cells with pronounced straight stress fibers (*e.g.*, polarized fibroblasts) have been found to orient longitudinally on cylinders, while cells with circular actin bundles (*e.g.*, epithelial cells) or cells with insufficient or no stress fibers (*e.g.*, transformed L fibroblasts) bend around the cylinder with much lower elongation and longitudinal orientation (Fig. 3a) [59]. While this theoretical explanation provides an interesting mechanistic perspective, it cannot elucidate all the aspects at play in stress fiber orientation. For example, in experiments on convex cylinders ($K = 0,\ H > 0$) with fibroblasts and smooth muscle cells, two distinct stress fiber populations have been observed that are not predicted by this theory: a set of long, apical stress fibers located above the nucleus and a set of shorter, basal stress fibers situated beneath the nucleus [57]. The apical and basal stress fibers increasingly align in axial and circumferential directions respectively with increasing curvature [57]. Interestingly, the circumferentially aligned stress fibers lie underneath the nucleus, while it might be expected from the theoretical explanation that they should lie close to the upper side of the cell to maximally compensate for the extension caused by cell bending. It, therefore, seems likely that predicting the energetically optimal orientation of cells encompasses more aspects than cell contractility and stress fiber bending.

Cells have no way to “avoid” curvature on convex spherical caps ($H > 0,\ K > 0$). In other words, the stress fibers in cells adhering to such spherical substrates must bend regardless of their orientation. Bone marrow stromal cells seeded on convex spherical caps were found to exhibit lower F-actin levels (*i.e.*, less pronounced stress fibers), yet higher phosphorylated myosin levels, indicative of higher myosin II filament activity as compared to the cells residing on convex cylindrical substrates of the same diameter [61]. It has been suggested that these increased phosphorylated myosin levels are necessary to compensate for the lower number of stress fibers whose formation seems to be impeded on convex curved substrates, such that an adequate cytoskeletal tension and cell motility could still be maintained [61]. This observation has been confirmed in other studies, where less pronounced, shorter stress fibers or lower F-actin levels were observed on the convex spherical caps as compared to other geometries in the surroundings [30,67,69]. From a curvature perspective, one expects a concave spherical pit ($K > 0,\ H < 0$) to elicit the same response, since there is also no direction of zero principal curvature ($K > 0$ on the concave and convex sides). However, there is a way in which cells could still avoid stress fiber bending: by spanning the pit with strong actin bundles, attached to a few anchoring points on the side walls, that contract and lift the cell body away from the substrate. Indeed, mesenchymal stromal cells cultured on spherical pits or inside spherical confinements form large extensions to bridge the concavity underneath and adopt a spider-like morphology, with most focal adhesions being located at the anchoring sites on the periphery of the cells (Fig. 3b) [69,93]. A similar lift-off behavior has recently been observed for stromal cells on concave cylindrical substrates ($K = 0,\ H < 0$), and this has been linked to the non-aligned, non-persistent migration behavior that these cells exhibit [63]. The spider-like morphology is reminiscent of the shape of cells on micropatterned adhesive substrates, exhibiting arc-like boundaries that form naturally due to cellular contractility (Fig. 5c) [94,95]. Cells on smooth, double-sinusoid substrates (varying K and H) seem to exhibit a somewhat similar behavior: the nucleus is typically positioned in a valley ($K > 0,\ H < 0$), and most focal adhesions are situated on the surrounding hills ($K > 0,\ H > 0$), though some more stable, higher tensioned FA could be present in the valleys [52]. Lower nuclear compression has been observed in the valleys, yet it is unclear if the cells were fully lifted away from the double-sinusoid substrate.

Based on these results for convex and concave spherical geometries ($K > 0$), a natural question to ask is what happens to the actin organization when cells are subjected to both convex and concave curvatures simultaneously (*i.e.*, saddle surfaces $K < 0$)? On the saddle-shaped region of sphere-with-skirt substrates, two distinct subpopulations of stress fibers have been observed in fibroblasts: apical stress fibers (above the nucleus) that align in the radial direction, and basal stress fibers (below the nucleus) that align in the circumferential direction. Interestingly, the apical stress fibers do not follow the local concave curvature of the substrate but bridge this concavity instead, much like the previously described spanning behavior on concave pits (Fig. 3c) [30]. Therefore, by aligning along the concave principal direction ($\kappa_1 < 0$) and consequently spanning the substrate, the apical stress fibers can avoid bending. The basal stress fibers, however, do not avoid bending and are oriented in the other principal (convex, $\kappa_2 > 0$) direction, showing a similar behavior as on cylindrical substrates in a previous study [57]. Therefore, while the argument of bending avoidance seems to hold for the apical stress fibers, it does not explain the orientation of the basal stress fibers: why do the basal fibers align in the “most curved” direction instead of trying to avoid curvature altogether? Elucidating the underlying mechanisms requires further investigation, but it is noteworthy that the cells cultured on the saddle region migrate in the direction of the basal stress fibers, while they typically migrate in the direction of the apical stress fibers on planar substrates [30]. Migration and basal stress fiber orientation may, therefore, be linked on those regions of negative Gaussian curvature.

The effects of cytoskeletal mechanics can be studied more in-depth by using drugs to inhibit or enhance specific cell components. Activation of Rho GTPases (*i.e.*, regulators of stress fiber formation [96]) in fibroblasts and vascular smooth muscle cells on the outside of cylinders ($K = 0,\ H > 0$) results in a strong reduction of apical, longitudinally aligned stress fibers, while basal stress fibers become more pronounced and align circumferentially [57]. While the opposite was expected (following the stress fiber bending argument), it has been hypothesized that this observation is due to a shift in the balance between the bending energy of stress fibers and cell contractility [57]. Rho inhibition, on the other hand, results in the loss of the curvature sensing ability of mesenchymal stromal cells cultured on double-sinusoid substrates (with varying K and H) [52]. A similar effect is obtained by drug-induced actin depolymerisation and myosin II blocking, both of which are among the components of the actomyosin contractile apparatus [52]. These results underpin the intimate connection between the formation of a contractile cytoskeletal structure and the ability of the cells to sense and respond to substrate curvature. While the full set of the mechanisms behind curvotaxis are not yet fully uncovered, the experimental observations seem to support at least some aspects of the hypothesis that cytoskeletal (and cellular) alignment is driven by an

energetic balance between contractility and stress fiber bending on curved substrates.

3.3. The nucleus as a curvature sensor and regulator

Located in between the cytoskeletal network of eukaryotes is the cell nucleus, the largest organelle that contains the cell's genetic material. Mechanically, the nucleus is a membrane-bound structure that is internally supported by a fibrous network-like nucleoskeleton, built up of lamins, actin, and other proteins [97,98]. The nucleus behaves like a viscoelastic solid [99], and is considerably stiffer than the cytoskeleton [98,100]. Nevertheless, it is still a deformable structure, and nuclear shape and deformability have been shown to play a role in various cell processes, including the regulation of gene expression, and have been associated with various diseases (*e.g.*, laminopathies) [100–102]. The deformation of the nucleus is enabled through intimate connections between the nuclear envelope and the cytoskeleton in the form of the LINC (linkers of nucleus and cytoskeleton) complex [103]. On the outer side of the nuclear envelope, nesprin proteins bind to the various components of the cytoskeleton: nesprins 1/2 bind to actin, nesprin 3 binds to intermediate filaments, and nesprin 4 to microtubules. At their other ends, nesprins bind to SUN proteins, which pass through the nuclear envelope and bind to nuclear lamins (proteins that form a reinforcing layer on the inner side of the nuclear membrane). These lamins are, in turn, connected to the chromatin cargo inside the nucleus [102,104]. Hence, there is a mechanical connection between the cytoskeleton and the nucleus, enabling force transmission of intracellularly and extracellularly generated forces [102]. This force transmission results in dynamic deformations of the nucleus, which have been linked to different mechanotransduction mechanisms. For example, nuclear deformation could result in conformational changes of proteins at the nuclear lamina, affecting their interaction with enzymes [105]. Additionally, nuclear deformation could rearrange the spatial distribution of chromatin (into loose and compact regions), affecting gene expression [101,104–106]. For these reasons, the cell nucleus could actually be considered a “sensor” that plays an important role in mechanotransduction [13,104].

The nuclei of certain cells (*e.g.*, fibroblasts) adhering to flat surfaces are naturally flattened due to the presence of a “perinuclear actin cap”, which is a dome-like arrangement of apical stress fibers that lie on top of the nucleus and that exert a compressive force on the nucleus due to actomyosin contraction [107] (Fig. 3e top row). Alterations in the shape of the nucleus are, therefore, expected to arise in the cells residing on curved substrates as compared to those cultured on planar substrates, due to the curvature-induced cytoskeletal rearrangement and the cell morphology that we described previously. Indeed, the nuclei of mesenchymal stromal cells seeded on planar ($K = 0,\ H = 0$), convex spherical ($K > 0,\ H > 0$), or concave spherical ($K > 0,\ H < 0$) substrates exhibit distinctly different shapes: a flattened morphology on flat and convex spherical substrates and a more spherical morphology on concave spherical substrates [69]. For a cell on a planar substrate, the perinuclear actin cap generates a relatively small compressive force, flattening the nucleus. On a convex spherical cap ($K > 0,\ H > 0$), however, this vertical force component increases due to the increased vertical arrangement of the stress fibers, leading to a more flattened shape. On a concave spherical pit ($K > 0,\ H < 0$), on the other hand, the nuclear compression is relieved because the cell is lifted off the surface, leading to a more spherical shape of the nucleus (Fig. 3e) [52,69].

One of the primary components governing nuclear deformability is lamin A. This is a type V intermediate filament that is a key constituent of the nuclear lamina, a reinforcing meshwork at the nuclear envelope [102,108]. Increased lamin A intensity levels have been measured in cells on convex spherical substrates, as opposed to concave spherical and flat substrates, suggesting a nuclear stress-protection response induced by curvature [69]. On the other hand, active lamin A silencing using small interfering RNAs has been shown to significantly reduce the curvature-sensing ability of cells [52]. In addition to nuclear deformation due to curvature-induced forces, the nucleus has also been found to dynamically change its intracellular position in response to curvature, essentially positioning itself in the locations of low deformation (*i.e.*, valleys instead of hills) and potentially playing an important role in guiding cell migration [52,68].

Curvature-induced deformation of the nucleus has also been linked to gene expression and differentiation. On substrates with a zero Gaussian curvature (*i.e.*, cylindrically-shaped hydroxyapatite substrates), no curvature-induced changes in the differentiation and mineralization rates of pre-osteoblast cells have been observed (using RUNX2, ALP, DMP1 and Osteopontin markers) [64]. However, curvature-dependent differentiation behavior has been observed on substrates with non-zero (positive) Gaussian curvatures [69]. Higher osteocalcin levels, a marker for osteogenic differentiation, were observed in MSCs seeded on hemispherical caps as opposed to flat and hemispherical pits (both in expansion and osteogenic medium) [69]. Remarkably, these higher osteocalcin levels were associated with lower F-actin levels and vice versa, while previous results on planar substrates indicated that higher cytoskeletal forces enhance osteogenic commitment [109]. This difference could indicate that surface curvature plays an equally important role in governing nuclear deformation, next to the magnitude of cytoskeletal tension. Nuclear deformation might also explain the lack of increased differentiation activity on cylinders as opposed to hemispherical caps: on the cylindrical substrates ($K = 0$), the stress fibers orient in the longitudinal direction and, therefore, might not compress the nucleus as much as on hemispherical caps ($K > 0$), and, thus, may not trigger the osteogenic pathways. The transcriptome of MSCs cultured on double-sinusoid substrates (varying K and H) has also been compared to that of the cells cultured on planar substrates ($K = H = 0$), showing several downregulated genes in cells on the sinusoid substrates, including factors involved in differentiation and cytoskeletal remodeling [52].

In conclusion, it should be clear that individual cells could sense and respond to various types of substrate curvatures (see Table 1 for an overview of studies on cell-scale curvature guidance). While generating and sensing curvature at membrane scale involves dedicated biochemical pathways and proteins at the membrane [10,46,47,51], the interaction with curvature at larger scales requires a more holistic, mechanical explanation [52]. In general, the mechanisms driving spatiotemporal organization of individual cells on curved substrates seem to be governed by the interplay between the cell's contractile apparatus and the relatively stiff, yet deformable nucleus [19,52,69]. By means of protrusions at their periphery [30], cells dynamically explore the 3D curved substrate and establish discrete focal adhesion sites, enabling them to anchor to the substrate, remodel their cytoskeleton, and build up cellular tension. This cytoskeletal contraction, in conjunction with the specific geometry that the cell is constrained to (*e.g.,* convex or concave spherical pits), results in different net forces on the nucleus as opposed to cells adhering to isotropic flat substrates. As a first consequence, these anisotropic force distributions could result in intracellular nuclear sliding, potentially driving whole-cell migration in a particular direction [52]. Additionally, the specific substrate that cells adhere to could result in varying degrees of nuclear compression, affecting chromatin distribution and potentially triggering other nuclear pathways [61,69]. The preferred orientation and migration trajectory that the cells then commit to, is typically discussed from an energy minimization perspective. Although it is still unclear to what extent different cell components contribute to the energy balance, it has been argued several times that stress fiber bending plays a major role [57,92]. Indeed, cells with pronounced stress fibers seem to favor orientations that minimize bending, such as a longitudinal alignment on convex cylinders or a “spanning” configuration over local concavities (*e.g.*, on concave pits, concave cylinders or saddles) [60,63]. While the full set of the involved mechanisms remains elusive, it should be clear

Table 1
General overview of cell-level curvature guidance studies, showing substrate type, curvature classification, scale, materials, cell types and key observations. Radius of curvature is denoted as r_c, wavelength and amplitude of sinusoidal substrates are denoted as λ and A respectively. Material abbreviations are as follows: PDMS = polydimethylsiloxane, PTMC = poly(trimethylene carbonate), PLGA = poly(lactic-co-glycolic acid), gelMA = gelatin methacryloyl.

Substrate type	K	H	Curvature scale (μm)	Materials	Cell type	Key observations
Convex cylinders	$K = 0$	$H > 0$	r_c= 5-15 [54] r_c= 18 [58,60] r_c= 12-25 [59] r_c= 5-121 [78] r_c= 150 [61] r_c= 40-200 [57] r_c= 125-500 [63] r_c= 220 [77]	Glass [54,57–60,77] PDMS [61,63] PLGA [78]	Fibroblasts [54,57–59,77,78] VSMC [57] Epithelial cells [58–60] MSC [61,63]	Longitudinal alignment [54,57–61,63,77,78] Transverse alignment [58–60]
Concave cylinders	$K = 0$	$H < 0$	r_c= 50-250 [64] r_c= 125-500 [63]	PDMS [63] Hydroxyapatite [64]	MSC [63] Osteoblasts [64]	Substrate spanning [63] Individual random alignment, collective longitudinal alignment [64]
Convex hemispheres	$K > 0$	$H > 0$	r_c= 10 [68] r_c= 50–150 [70] r_c= 125–375 [69] r_c= 250–2000 [67]	Glass [67] PDMS [68,70] PTMC [69]	MSC [67,69,70] Macrophages [68] Fibroblasts [70]	Increased nuclear deformation, osteogenic differentiation [69]
Concave hemispheres	$K > 0$	$H < 0$	r_c= 10 [68] r_c= 50–150 [70] r_c= 125–375 [69]	PDMS [68,70] PTMC [69]	Macrophages [68] MSC [69,70] Fibroblasts [70]	Substrate spanning [69] Escape from concave wells [70]
Saddle	$K < 0$	$H \neq 0$	r_c= 375 [63]	PDMS [63]	MSC [63]	Substrate spanning and migration in concave direction [63]
Sphere-with-skirt	$K_{min} < 0 < K_{max}$	$H_{min} < H < H_{max}$	r_c= 80–500 [30]	PDMS [30]	Fibroblasts [30]	Avoidance of spherical cap, perpendicular alignment of SF subpopulations on saddle-shaped region [30]
Single sinusoidal sheet	$K = 0$	$H_{min} < 0 < H_{max}$	λ= 200, A = 40 [65] λ= 20–160, A = 10 [66]	GelMA [65] PUA [66]	Myoblasts [65] T cells [66]	Longitudinal alignment [65] Longitudinal, zigzagging migration [66]
Double sinusoidal sheet	$K_{min} < 0 < K_{max}$	$H_{min} < 0 < H_{max}$	λ= 30–300, A = 1–30 [52]	PDMS [52]	MSC [52]	Migration to concave valleys, avoidance of convex hills [52]

that cell-scale curvature guidance is not purely a biochemical process that is restricted to specific regions inside the cell, but instead requires a whole-cell approach involving the interplay between the cell as a dynamic mechanical system and the constraining extracellular geometry.

4. Collective cell and tissue response to substrate curvature

While single-cell experiments offer useful insights into the mechanisms behind curvature sensing and response, cells are generally not solitary agents *in vivo*, but are, instead, linked together in a multicellular network [11]. This could be a direct link through intercellular connections such as tight junctions, gap junctions, desmosomes, and adherens junctions [11], or an indirect connection via cell-ECM adhesion [88,110]. These cell-cell and cell-ECM interactions establish a mechanical linkage that enables force transmission between different cells. As mentioned before, cell-ECM force transmission involves transmembrane integrins that bind to extracellular matrix ligands and link back to the cell cytoskeleton [111]. In the case of cell-cell interactions, a similar force transmission mechanism exists, this time mediated by transmembrane cadherins [88]. The extracellular domains of the cadherins of different cells form adhesive bonds that link the cells together. At the cytoplasmic domain of the cadherins, different proteins are recruited, such as α-catenin, β-catenin, or vinculin, that enable direct or indirect binding to actin [88,112]. As such, a mechanical connection between the cytoskeleton of different cells is constructed. Through these cell-cell and cell-ECM connections, a multicellular force-feedback network is established that increases the range within which cells could sense and respond to their environment, enabling them to act cooperatively [19]. For example, collective cell contraction on patterned adhesive islands or confinements could result in stress gradients in the multicellular constructs that drive spatial cell proliferation patterns [37] and the spatial distribution of biochemical signals [23]. Hence, the collective force-generation of multicellular systems coupled with constraining extracellular geometries could initiate heterogeneous cell patterning and guide the structural organization of the extracellular matrix [19]. In the current section, we approach this coupling between collective cell action and extracellular geometry from the perspective of substrate curvature, first by discussing the response of single-layer cell sheets and later by considering the shaping of more convoluted ECM-rich tissues.

4.1. Curvature-driven organization and dynamics of cell sheets

Upon reaching confluence, cells link up to form a cohesive cell sheet, or monolayer, that covers the substrate they are situated on. At this moment, cells can operate collectively, for example, to generate forces across the entire sheet [110]. While various cell types could form monolayers, most studies of monolayer mechanics and structure are focused on epithelial cell sheets, which have a high physiological relevance, since they line the surfaces of many 3D curved structures *in vivo*, such as organs, cysts, and vessels [113,114]. In addition to inducing, for example, spatial proliferation patterns, the collective organization can enable cells in monolayers to sense and respond to weaker curvature fields than individual cells. Indeed, confluent monolayers of fibroblasts and vascular smooth muscle cells residing on cylindrical substrates ($K = 0,\ H > 0$) align along the cylinder axis more strongly than individual cells on cylinders with low curvature (Fig. 4a) [57]. As a potential explanation, it was suggested that these monolayers have a larger “effective length scale” due to the cell-cell connections that link stress fibers together, thereby creating a stress fiber network that has a higher bending energy penalty than in individual cells [57]. Cylindrical geometries also play an important role in the organization and dynamics of epithelial and endothelial sheets (*e.g.*, during tubular morphogenesis) [115]. Indeed, cells in such monolayers plated on cylindrical substrates align and elongate in response to curvature, although the orientation and curvature sensitivity depends on the cell type. Longitudinal alignment is observed for umbilical vein endothelial cells cultured on convex cylinders ($H > 0$) and renal epithelial cells in concave cylinders ($H < 0$), while renal epithelial cells align perpendicularly to the cylinder axis on convex cylinders (Fig. 4b) [80,116–118]. The curvature sensitivity seems to be reduced in cell sheets with stronger cell-cell junctions and/or higher cell stiffness, which has been linked to an organ-dependent requirement to minimize paracellular transport (*e.g.*, in the blood-brain barrier) [116,117]. On double-sinusoid substrates with varying, non-zero Gaussian curvatures, an expanding epithelial monolayer showed curvature-dependent organization at the leading edges of the front, where cells are positioned in the concave areas, but not in the central part [52]. As a potential explanation, it was suggested that the cells at the edges of the expanding colony have a higher freedom to reposition themselves in response to curvature, while the cells in the center part do not have such freedom due to cell-cell interactions which provide constraints on the position of the cell within the epithelium [52].

When organized in monolayers, cells also exhibit a collective migration behavior that plays a crucial role during morphogenesis, wound healing, and cancer progression, and has been found to depend on substrate curvature [73,119,120]. Epithelial cell sheets on the outside of cylindrical wires ($H > 0$) migrate collectively in the longitudinal direction, and the migration speed increases with curvature [80]. On the inside of hollow cylindrical substrates ($H < 0$), however, the migration speed of an advancing epithelium decreases with increasing curvature, potentially due to cell jamming (Fig. 4c) [114,118]. Moreover, cells can detach from the front edge of the monolayer on cylindrical substrates at high curvatures, and switch to an individual migration mode, a phenomenon that is reminiscent of epithelial-to-mesenchymal transition [80,121]. Despite ample evidence showing that curved substrates guide cell sheet organization and migration, this does not mean that the sheet maintains this geometry for extended periods of time [122]. Instead, cell sheets can detach from concave cylindrical substrates ($H < 0$), a phenomenon that is more profound for increased curvatures and increased cell contractility and can be explained by the existence of a net normal stress pointing away from the surface (Fig. 4d) [122,123]. Cell sheet detachment is not limited to cylindrical geometries, but can also occur on substrates with non-zero Gaussian curvatures. For example, epithelial cell sheets grown in bent cylindrical tubes, effectively representing a portion of a torus with $K < 0$ at the inside and $K > 0$ at the outside of the bend, consistently detach from the outer side of the bend as a consequence of cell sheet contraction (Fig. 4e) [123]. Moreover, cell sheet contraction can cause initially planar substrates to buckle into spherical-like microlenses ($K > 0$), hence giving rise to spontaneous curvature formation [124].

Substrate curvature not only influences the organization, migration, and detachment of entire cell sheets, but can also affect individual cells within the sheet. More specifically, recent evidence has shown that some cells in a curved epithelium must adopt a previously unknown mathematical shape, termed a scutoid, in order to geometrically enable the packing of cells in such a curved morphology (Fig. 4f) [125]. Similar to a prism and a frustum, a scutoid is a polyhedron connecting two parallel polygonal faces. In contrast to the prism and frustum, however, a scutoid connects different polygons at the top and bottom (*e.g.*, a hexagon on top and a pentagon on the bottom, Fig. 4f). Previously, it was assumed that epithelial cells adopt a prism or frustum shape in a closely-packed epithelial sheet [126,127]. Mathematical models, however, revealed that certain cells in a curved epithelium have different neighboring cells at the apical and basal sides, necessitating scutoid shapes in the epithelial packing rather than only prisms and frusta [125].

4.2. Curvature-dependent, fluidic shaping of ECM-rich tissues

Cell sheets could, thus, exhibit complex shape formation and adaptation in response to geometrical cues in their environment.

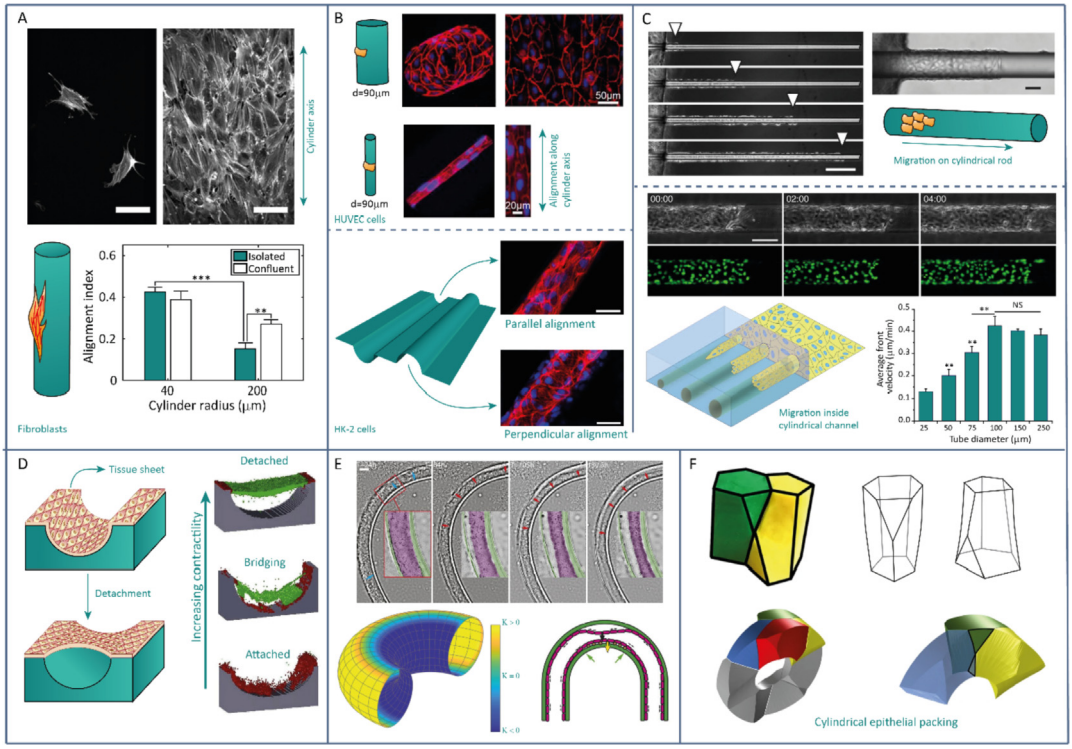

Fig. 4. The response of cell sheets to the substrate curvature. a) A confluent layer of fibroblasts senses substrate curvature better than individual cells, obtained with permission from Ref. [57]. b) Top: human umbilical vein endothelial cells (HUVEC) show increasing alignment in the longitudinal direction on cylindrical substrates, obtained with permission from Ref. [116]. Bottom: human kidney (HK-2) epithelial cells showing different alignments on concave and convex hemicylindrical substrates, obtained with permission from Ref. [117]. c) Top: the collective migration of an epithelium on the outside of a cylindrical wire, obtained with permission from Ref. [80]. Bottom: the collective migration of an epithelium inside cylindrical channels, with decreasing speeds for increasing curvatures, obtained with permission from Ref. [118]. d) A schematic drawing of cell sheet detachment in response to the substrate curvature, reproduced with permission from Elsevier [122]. e) An epithelium cultured inside a bent cylindrical tube, detaching from the outer side (positive Gaussian curvature). Experimental images and inset on the right were reproduced with permission from Ref. [123]. f) The scutoid cell shapes emerging in a cylindrical epithelial packing, obtained with permission from Ref. [125].

Moreover, spatial force patterns or mechanical instabilities arising from differential growth further contribute to shape formation in cell sheets, as was already mentioned in Section 2.2 in connection to morphogenesis and pathology [24,31,32,37]. Such complex shape formation is, however, not restricted to cell sheets but could also be observed in 3D bulk tissue constructs in which extracellular matrix is gradually deposited as 3D tissue grows. This matrix reinforces the cell collective and enhances the load-bearing capacity of the developing tissue [128]. Despite the fact that a dense cell-ECM network is formed, these tissue constructs still exhibit geometry-dependent, fluid-like shape formation [129]. The effects of geometry in general and curvature in particular on the shape and kinetics of tissue growth has been studied primarily using osteoid-like tissues as model systems [129–131]. This is likely driven by the clinical demand for geometrically optimized porous biomaterials that facilitate bone tissue regeneration. Typically, curvature-guided tissue growth has been studied *in vitro* and has involved non-mineralized (osteoid-like) tissue, although *in vivo* curvature guidance of mineralized tissue has been also recently reported [132]. In the current section, the general observations regarding curvature-guided tissue growth will first be outlined, after which the physical basis for this behavior will be discussed by comparing it to surface tension-driven shape formation in inanimate materials.

Following the seminal work of Rumpler et al. [130], several *in vitro* studies involving pre-osteoblasts or mesenchymal stromal cells seeded inside straight channels with pre-defined pore shapes have consistently revealed that the curvature of the pores affects the shape and kinetics of tissue growth (Fig. 5a) [130,131,133–138]. More specifically, after an initial stage that is dependent on cell-material interactions, pore curvature becomes the dominant factor for tissue growth [135]. In channels with circular pores, non-mineralized tissue has been found to grow uniformly inwards, with larger tissue thickness for higher curvatures (*i.e.*, narrower pores) [130,133,134], and similar results have been obtained for mineralized tissue under static and perfused conditions [136]. In non-circular channels (*e.g.*, with triangular or square cross sections), preferential tissue growth starts in the pore corners (*i.e.*, the regions of high curvature), while no tissue is formed on the flat sides initially [130,131,135,138]. As tissue is progressively deposited in the corners, effectively rounding the pore, the local geometry of the flat sides is altered and tissue starts to grow on those locations too. With time, this leads to a circular tissue front that grows uniformly inwards. In channels with convex polygonal pores, the tissue growth rate in the corners increases with corner curvature, meaning that it is higher in the corners of triangular than in square or hexagonal pores [130]. Nevertheless, the average growth rate of convex pores with the same perimeter is independent of their shape, which has been attributed to the fact that, in convex polygons, the average curvature and, thus, average growth rate is inversely proportional to the perimeter [130,131]. However, in channels with concave polygonal cross sections such as cross shapes, the initial overall growth rate can be significantly higher than in square (convex) shapes, due to the higher number of "growth-inducing" corners in the cross (8 concave corners) as compared to the square (4 concave corners) shape [131]. This implies that the pore geometry of artificial tissue scaffolds should be optimized not only for mass transport and mechanical properties, but also for the desired tissue growth rate [131].

These straight pore channels, whether with convex or non-convex cross-sectional shapes, all classify as "generalized cylinders" (*i.e.*, developable geometries, $K = 0$) with parallel ruling lines that are curved in one direction but remain flat in the other. Other examples are hemicylindrical, open channels, or wavy substrates that only curve in one

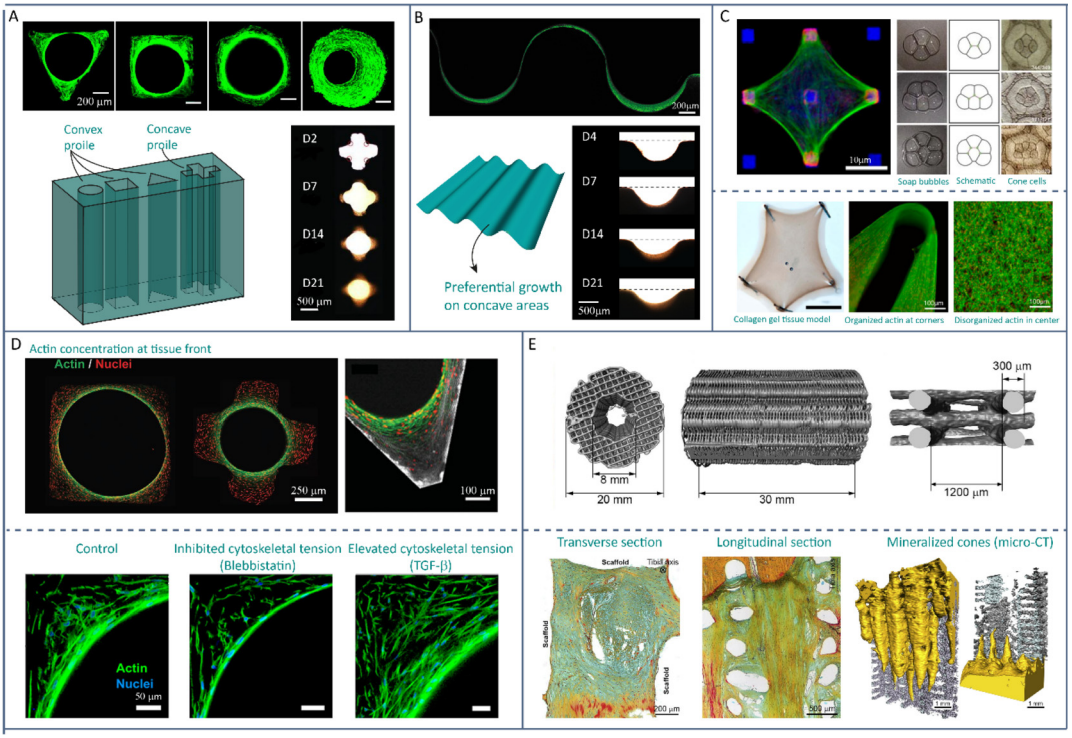

Fig. 5. Curvature-driven tissue growth. a) Bone-like tissue growth front evolving towards a circular geometry in pore channels with various cross-sectional shapes. The experimental images on top and on the right are obtained with permission from Ref. [130] and Ref. [131], respectively. b) The differences in the bone-like tissue growth on concave cylindrical versus convex cylindrical regions. The experimental images on top and on the right are obtained with permission from Ref. [139] and Ref. [134], respectively. c) Surface tension determines confined cell and tissue shapes. Top left: A buffalo rat liver cell on a micropatterned adhesive substrate, obtained with permission from Elsevier [146]. Top right: similarity between clustering soap bubbles and cone cells in the developing *Drosophila* retina, obtained with permission from Springer-Nature [140]. Bottom: Tension-driven shape adaption of a collagen gel tissue model pinned at discrete locations, obtained with permission from Elsevier [146]. d) Actin alignment and increased concentration at the tissue front. Experimental images obtained with permission from Ref. [131] (top left), Ref. [138] (top right) and Ref. [148] (bottom). e) Top: additively manufactured scaffold implanted in a critical-sized defect in an ovine animal model. Bottom: Soft tissue growth towards cylindrical pores (left and middle), and mineralized cones as obtained with microcomputed tomography (right). Images are obtained with permission from Elsevier [132].

direction. A general and important observation regarding such geometries is that the tissue is predominantly formed on concave regions ($H < 0$), with virtually no (initial) tissue deposition on the convex regions ($H > 0$, Fig. 5b). In hemicylindrical channels, for example, tissue progressively grows in the concave part of the substrate, effectively "flattening" the cylindrical cavity, and the tissue front is pinned at the convex edges [131]. Moreover, the tissue grows at a significantly lower rate than in full cylindrical channels of the same radius, which is attributed to the presence of the convex boundaries on which no tissue is formed until the local geometry becomes concave due to the advancing tissue front [131]. On wavy substrates, exhibiting alternating patterns of convex and concave regions (*i.e.*, positive and negative mean curvatures), tissue is also almost exclusively generated inside the concave regions [134,139]. Similar results are seen inside prismatic channels with non-convex pores, such as a cross shape, where tissue starts growing from the concave corners and only forms on the convex corners once they become immersed in the advancing tissue front [131].

In most curvature-guided tissue growth studies, channel-like (*i.e.*, intrinsically flat, $K = 0$) substrates have been employed, and tissue growth has been typically quantified from a 2D perspective by using the projected tissue area perpendicular to the channel length [130,131,134,135,137]. However, the projected tissue area as seen from the top (or bottom) of the channel would only be an accurate measure of the total tissue formation, if the tissue growth is uniform along the depth of the channel, which might not be the case due to the non-uniform initial cell density or the disturbing presence of the convex boundaries [134]. Indeed, it has been suggested that the tissue growing in a cylindrical channel should exhibit curvature in both principal directions (*i.e.*, intrinsic curvature) and adopt a catenoid-like saddle shape ($K < 0$) [131], although the 3D reconstructions of *in vitro* grown mineralized tissue under static and perfused conditions could not confirm this hypothesis [136]. Nevertheless, it seems plausible that tissue could develop into more complex architectures than developable geometries ($K = 0$) and instead adopt intrinsically curved shapes ($K \neq 0$). It would, thus, be relevant to also study tissue growth on such intrinsically curved (sphere-like or saddle-like) geometries, yet surprisingly little research has been conducted in this direction. A recent study involving human corneal stromal cells seeded on shallow dome-like substrates ($K > 0$) shows that substrate curvature enables the formation of highly aligned extracellular matrix in the radial direction, giving rise to tissue equivalents that resemble many of the characteristics of natural corneal tissue [81]. In another recent study, osteoid-like tissue was grown from pre-osteoblasts on saddle-shapes with controlled curvature [129]. More specifically, the tissue was formed on rotationally symmetric capillary bridges of constant mean curvature and non-constant negative Gaussian curvature. The saddle-shaped tissue front is pinned by the convex edges of the substrates and progressively extends outwards, effectively flattening the initial geometry. Accordingly, the final tissue thickness is higher on substrates with narrow neck regions (*i.e.*, higher concave principal curvature and higher Gaussian curvature) [129]. These intriguing initial results call for more detailed investigations into tissue growth on intrinsically curved geometries, both spherical and hyperbolic, as these bear significant physiological relevance.

It should, thus, be clear that the shape of newly formed, ECM-rich tissue depends on the geometry, more specifically curvature, of the underlying substrates. But why does tissue adopt these particular

shapes? A consistent observation that could elucidate this matter is that the tissue shapes are reminiscent of the shapes that viscous fluids would adopt, as dictated by the laws of physics [19]. In other words, the emergent shape of biological materials is somewhat similar to observations made in physics-driven inanimate materials, such as wetting droplets, soap bubbles, or other systems involving liquid interfaces. For example, the pattern formation of cone cells in the developing *Drosophila* retina exhibits a striking similarity to soap bubble clustering (Fig. 5c) [140]. The underlying physical mechanism driving shape formation of these inanimate materials is the minimization of surface or interfacial tension, resulting in a tendency to minimize the surface area [20]. Due to the apparent similarity between the liquid and biological shape formations, on long enough timescales, tissues are said to behave like viscous liquids with a certain surface tension [141–143]. As such, the emergent organization of tissue on curved substrates is often attributed to surface tension minimization, although other factors are at play as well [19,144]. The relation between the shape and surface tension is governed by the Young-Laplace equation [145], which states that the pressure difference (Δp) sustained across a fluid interface is proportional to the surface tension (σ) and the mean curvature (H):

$$\Delta p = 2\sigma H \tag{4}$$

Indeed, the Young-Laplace equation, or a slightly modified version thereof, has been employed to describe the shape of cells and tissues pinned at discrete sites on a flat substrate [146,147], but also that of the osteoid-like tissue grown on intrinsically curved substrates [129]. While tension in a liquid results from various intermolecular cohesive interactions (*e.g.*, van der Waals forces), the origin of tissue tension has been explained using different theories, such as the “differential adhesion hypothesis”, but seems to involve both intercellular adhesion and cortical contractility [141,142]. Indications of interfacial tension in the *in vitro* curvature-driven growth of connective tissue are provided in the form of strong actin fibers that are highly aligned with the tissue-medium interface [130,131,133–135]. Moreover, the actin density is higher close to the tissue-medium interface, despite uniform cell density throughout the tissue bulk (Fig. 5d) [131,134]. It has been hypothesized that the collective alignment of actin at the tissue front could result in a net normal force pointing away from the surface, thereby driving further advancement of the tissue front [133]. Additionally, the high tension that exists at the growth front can induce cell transitions, such as a reversible transition between fibroblasts and myofibroblasts that is essential in wound healing [148]. In addition to cell-scale actin orientation, the collagen fibers in the synthesized extracellular matrix follow the same alignment, indicating also tissue-level organization [131]. In fact, the tensile forces generated by cytoskeletal contractions are gradually transferred to the collagen fibers as tissue progresses, resulting in a permanently stressed matrix that can partly take over some of the cell-generated tension [138]. On saddle-shaped substrates ($K < 0$), actin fibers have been shown to exhibit chirality and align roughly in the direction of local zero curvature [129]. This could potentially indicate an energetically favorable orientational order in line with the recent hypotheses that tissues can behave like active nematic liquid crystals, with cells being the nematic agents, although more evidence is required to confirm this hypothesis [129,149].

Most curvature-driven tissue growth studies have been performed *in vitro*, yet some *in vivo* results also indicate that curvature plays a role in the organization and kinetics of tissue formation. In strut-based scaffolds used for the treatment of large bone defects *in vivo*, fibrous tissue formation has been found to be guided by the scaffold geometry with fibers aligning and spanning between cylindrical struts [150]. Furthermore, newly formed blood vessels were found to be primarily situated in the concave regions ($H < 0$) of a bone implant in the initial stages after implantation, potentially indicating curvature-guided angiogenesis during bone regeneration [151]. Using a scaffold with horizontal struts in a 0/90° pattern, it was recently shown that scaffold curvature drives soft tissue formation *in vivo*, and a novel matrix mineralization process was observed (Fig. 5e) [132]. More specifically, tissue growth was initiated at the scaffold regions of high mean curvature, and could be predicted effectively using a curvature-driven tissue growth model (Fig. 7c) [132].

In conclusion, it should be clear that the interplay between mechanics and geometry extends beyond the level of individual cells, and also plays an important role in shaping more complex, multicellular tissue constructs. In the case of single-layer cell sheets, such as epithelial monolayers, the balance between substrate curvature, cell-cell adhesion, and collective sheet contraction could affect collective migration [80,118], sheet detachment [122,123], or even the shape of individual cells [125]. Additionally, these thin cell sheets could buckle, wrinkle, or fold from a flat state into complex, curved shapes in response to externally applied loads (potentially balanced by internal prestress [152]). In the case of ECM-rich tissues, such as osteoid-like tissues, an apparent liquid-like behavior is observed as the tissue grows in a 3D (curved) environment. In general, such tissues grow preferentially on concave areas (*e.g.*, in the corner regions of straight-sided pores) causing a gradual smoothing in the extracellular geometry that is sensed by new cells [130,134]. These growing tissues exhibit cells with aligned actin fibers (primarily at the tissue front) [131]. Similar alignments are also observed in the ECM fibers that are deposited [138]. The liquid-like shape-formation observed in these ECM-rich tissues has, consequently, been linked to the concept of surface tension [129]. Mechanical principles, therefore, seem to govern much of the shape formation at the tissue level in a manner similar to the spatio-temporal organization of single cells on curved substrates. While force-transmission and long-range cytoskeletal remodeling through cell-cell or cell-ECM interactions undoubtedly plays a key role in this emergent organization, more insights are required to uncover how cell-level organization translates to tissue-level organization.

5. Computational models for curvature guidance

In addition to *in vivo* and *in vitro* experiments, the role of substrate curvature on the cell and tissue response could be elucidated further using *in silico* models. Computational approaches are particularly relevant for the design and optimization of artificial tissue scaffolds, and their importance is expected to increase significantly in the future [153]. Many phenomenological and mechanistic theoretical models capable of predicting experimentally observed behavior have been developed on various scales. Here, we aim to highlight those models that have been specifically directed at modelling the behavior of cells and tissues on curved geometries, and we refer to other reviews for a broader perspective on the *in silico* models of cells and tissues [19,154,155].

5.1. Cell-scale models

Mathematical models of the cell, either discrete or continuum, have been developed to describe and predict a variety of cell-scale processes, including cell contractility [156], focal adhesion formation [157], or migration [158]. Given the relatively recent interest in cell-scale curvature guidance, however, theoretical models that specifically address the effects of substrate curvature on single-cell response are not yet widespread. In one of the earliest models (briefly mentioned in Section 3.2, Fig. 6a), the cell body and stress fibers are respectively modelled as elastic plates and rods, and the stress fiber orientation is predicted by minimizing the total elastic energy of the system. Essentially, the orientation is determined by a competition between the bending energy of the stress fibers and the energy arising from cell contractility, the balance of which can be captured using a dimensionless parameter [92]. Consequently, the model is able to predict that fibroblasts, with a high stress fiber bending modulus, should align along the cylinder axis, while epithelial cells, with thin stress fibers, should align perpendicularly, in accordance with experimental results [59].

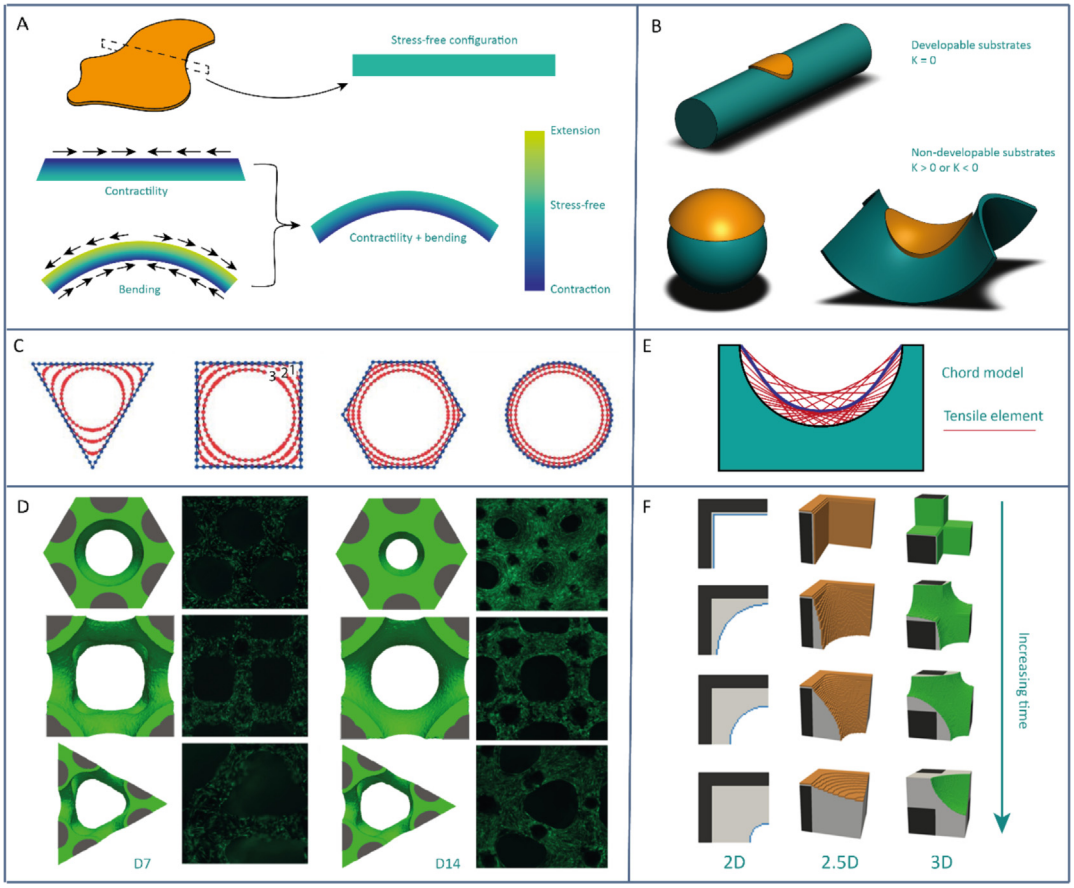

Fig. 6. Cell and tissue-scale computational models. a) A schematic overview of the through-thickness strain variation of a cell adhering to a convex cylindrical substrate, showing the combined effects of active contractility and cell bending. Adapted from Ref. [92]. b) A schematic illustration of a cell (orange) adhering to developable (top) and non-developable (bottom) substrates. The conformation of an initially flat cell to a non-developable substrate requires cell stretching or shrinking. c) Three consecutive evolutions of the tissue front as predicted by the curvature-driven growth model of Rumpler et al. Obtained with permission from Ref. [130]. d) 3D tissue growth predictions of a level-set curvature-driven growth model, with experimental images from *in vitro* grown bone tissue on day 7 (left) and day 14 (right), obtained with permission from Springer-Nature [167]. e) The geometrical chord model [134], representing tissue front evolution as an assembly of tensile elements. f) The predictions of a curvature-driven growth model (using a scanning mask) on different types of geometries, obtained with permission from Springer-Nature [170].

Another study implemented a phenomenological constitutive model based on a theoretical description of actomyosin contractility homogenized to the macroscale cell level in commercial finite element software to investigate the cytoskeletal stress distributions in the cells adhering to curved substrates [159]. According to this model, the substrate curvature can inhibit actomyosin contractility in two independent ways: through stress fiber bending, causing the contractile apparatus to perform sub-optimally, and through a pre-stress that arises when a flat cell should conform to a curved substrate. This last aspect is particularly interesting, as it allows delineating between intrinsically curved substrates (*i.e.*, spheres or saddles) and intrinsically flat substrates such as cylinders (Fig. 6b). On cylinders, the pre-stress is not present since an isometric transformation (*i.e.*, a transformation that does not require stretching) between a flat cell and the cylindrical substrate is possible. On spheres and saddles, however, the cell should locally stretch or shrink in order to conform to the substrate, a consequence of Gauss' "remarkable theorem" [21], giving rise to a pre-stress in the cell. The model, thus, dictates that contractility in cells on cylinders (or other developable substrates) is only impeded by the bending of stress fibers, while cell contractility on intrinsically curved substrates is affected by both the bending of stress fibers and a cellular pre-stress.

In a more recent numerical model, a discrete approach was employed where the cell is modelled as a tensegrity system (*i.e.*, a network-like structure containing isolated compression elements stabilized by tension elements) [160], using non-smooth contact dynamics [161]. Several intracellular components that are important in cell mechanics were explicitly implemented in the model, such as the cell membrane, focal adhesions, and the different types of cytoskeletal filaments. The non-smooth contact dynamics method treats the intracellular components as collections of rigid elements that interact with each other through contact, cable, or spring interactions [161,162]. The ensemble of all these components and their interactions then constitutes a model that, after calibration and verification using experimental data, enables the estimation of the forces and strains acting on all considered intracellular components in response to curved, perfectly rigid substrates. For example, the model predicts a more stable and rounder nucleus on concave ($K > 0,\ H < 0$) than on convex ($K > 0,\ H > 0$) hemispherical substrates, in accordance with some single-cell experimental results [52,69,161]. Furthermore, the discrete nature of the model enables the investigation of the relative importance of certain cellular components (*e.g.*, microtubules) on the overall mechanics, reminiscent of drug targeting that has been used experimentally to inhibit certain cell components [161].

Another recent discrete approach models cells on convex and concave cylindrical substrates as a collective of a deformable cell membrane, a solid spherical nucleus, and a string-like cytoskeletal structure [163]. By modelling temporary integrin-ligand bonds to account for the cell-substrate adhesion, and by calculating the protrusion forces created at the adhesion sites, the model aims to simulate the migration of the

cells residing on curved substrates. The purely mechanics-based model indicates that the curvature of the substrate provides a geometrical constraint on the protrusion force direction, meaning that it promotes protrusion in the longitudinal direction and consequent migration in that direction [163].

Despite capturing various experimental observations, these continuum and discrete models have, thus far, primarily provided qualitative insights on cell response to curvature. To a large extent, this is the consequence of the major assumptions that are necessary in the model development stage, either because the biophysical mechanisms are not yet fully understood, or to keep the model tractable. For example, most models assume that cells fully conform to the curved substrates, while experimental evidence seems to indicate that cells might lift off from some substrates [69]. Additionally, most models employ a purely mechanics-based approach, neglecting various biochemical processes, and typically consider a quasi-static situation, despite the dynamic behavior observed in the experiments [161]. Nevertheless, *in silico* attempts at understanding curvature-guided cell response are valuable for elucidating the importance of intracellular components, and their value will only increase when more of the underlying physical principles are understood and implemented.

5.2. Tissue-scale models

While single-cell models could eventually lead to a deeper understanding of the cell-scale mechanisms behind curvature-sensing, most theoretical efforts on this matter have been directed at the tissue level, often by means of phenomenological tissue growth models that consider a continuum or interfacial evolution perspective [19]. In most cases, these models are specifically used to predict bone tissue growth, although the components of the tissue (*e.g.*, collagen fibrils) are generally not explicitly modelled.

The simplest (and first) curvature-driven tissue growth model considers a 2D case, simulating tissue growing progressively inwards in pores with pre-defined cross-sectional shapes (Fig. 6c) [130]. In this type of phenomenological models, tissue is deposited only in concave regions ($\kappa \leq 0$), at a rate (ds/dt) proportional to the curvature (λ is a growth rate constant):

$$\kappa \leq 0\text{: } ds/dt = -\lambda\kappa \tag{5}$$

$$\kappa > 0\text{: } ds/dt = 0 \tag{6}$$

Despite its simplicity, this 2D growth law is able to replicate experimentally observed tissue growth (in terms of the projected tissue area) in various pore types remarkably well, showing the typical corner smoothing and the development of a circular growth front [130,133]. To a first approximation, the local curvature at discrete points along the pore can be estimated from the radius of the circumcircle that passes through each point and its two immediate neighbors [130]. In a more general version of the model, the local curvature is estimated using the Frette's algorithm [164], by sliding a circular mask across the scaffold-medium interface on binarized images and calculating the curvature as a function of the ratio of the pixels present on both sides of the interface [134,164]. This enables the simulation of tissue growth on the digital images of as-manufactured pore geometries, and facilitates consequent comparison with the corresponding experimental results [131,134]. The radius of the circular mask, defined in terms of the number of pixels, should be chosen appropriately (*e.g.*, in the order of the cell size), as it directly affects the curvature estimation. Furthermore, this growth law has no intrinsic time dependency. A time scaling is, therefore, necessary in order to match the experimentally observed tissue growth rates with the simulations [131,134]. Considering the evolution of the (projected) tissue-medium interface, this 2D curvature-driven growth law is in fact equivalent to the mathematical concept of curve-shortening flow, during which points on a smooth, closed curve move inwards perpendicularly, at a speed proportional to the curvature, thereby shortening the curve and decreasing the enclosed area [165]. Eventually, this causes convex and non-convex shapes to smoothen into a circle that uniformly shrinks towards a single point, reminiscent of the tissue front evolution observed experimentally [130,131,134,135].

The same type of growth law can be extended to 3D, by employing a spherical, voxelized scanning mask for curvature estimation rather than a circular mask (Fig. 6f) [166]. In this case, the tissue growth rate is taken to be proportional to the mean curvature, H, of the substrate and tissue is only deposited in concavities, with $H < 0$ (or $H > 0$ depending on the normal definition). Similar to the 2D case, the 3D implementation requires some fine-tuning of the mask diameter and time scale parameter, to achieve a realistic growth behavior that matches the experimental results. Additionally, in order to accurately model growth in the third dimension (*e.g.*, in a 3D pore channel), the volume scanned by the mask should progressively increase downwards, effectively simulating the migration of cells down the pore channel [166]. Instead of using a scanning mask for curvature estimation, a similar growth law could be implemented in a model that is based on the level set method [167]. This is a numerical approach to track the interface evolution between two domains, Ω_a and Ω_b, that has applications in diverse fields [168,169]. The level set function, ϕ, is defined to be zero on the interface between both domains, and non-zero inside the domains. By numerically solving an advection equation of the level set function, with an advection velocity that is proportional to the mean curvature, the evolution of tissue growth can realistically be simulated, albeit some time scaling is required to match the growth rate to the experiments. An important advantage of the level set method is its intrinsic curvature evaluation, eliminating the need for a scanning mask and the associated fine-tuning [167]. 3D growth models like these can be readily applied for the *in silico* investigations of tissue growth on various types of artificial scaffolds, thereby facilitating the optimization of scaffold geometries in terms of the predicted tissue growth behavior (Fig. 6d) [167,170]. Essentially, the tissue evolution predicted by these 3D growth models is intimately connected to the mathematical concept of mean curvature flow, which is a more general, higher-dimensional form of the curve shortening flow that could describe the 2D growth models [171]. The fact that mean curvature-driven growth models can capture experimental observations so well once more supports the idea that (apparent) surface tension plays a role in tissue front evolution, because the evolution of systems governed by surface tension, such as soap films, has been described using mean curvature flow. Moreover, such soap-film-like systems evolve towards energy-minimizing configurations in the form of minimal surfaces (*i.e.*, surfaces of zero mean curvature) [20,166]. Indeed, the natural structure of trabecular bone has been found to exhibit a mean surface curvature close to zero [42,43], which is why minimal surfaces have seen a surge of interest for the design of bone-substituting biomaterials [172]. While more research is needed to confirm that tissue, indeed, evolves towards a surface with $H = 0$ (recent results suggest it might evolve towards a constant, non-zero mean curvature configuration [173]), it is clear that surface tension plays an important role, and that models describing the interface evolution based on some applications of the mean curvature flow can yield realistic predictions.

In addition to the phenomenological models describing the interface evolution, attempts have been made at developing more mechanistic theories to describe tissue growth. For example, a thermodynamically admissible growth law for volumetric tissue growth can be constructed in terms of an eigenstrain that arises as new tissue is added to the bulk [174]. This continuum model, thus, predicts tissue growth as a function of the stress state that would be felt by the cells in the tissue. While still requiring some phenomenological input, the model can replicate the experimentally observed tissue deposition in circular pores, and predicts higher circumferential stress close to the tissue-medium interface, in line with the observations of strong actin signals at the interface [130,174]. By extending the growth law to incorporate the surface

stress in addition to the eigenstress, the model is capable of replicating the inhibition of tissue growth on convex as opposed to concave cylindrical substrates [139]. Alternatively, experimentally observed smoothing of the substrate and tissue growth slowdown could be simulated by modelling the changes in cell density and spreading due to curvature (volumetric crowding), and also accounting for cell diffusion and depletion [175,176].

Another mechanistic explanation builds upon a remarkably simple geometrical analysis in 2D, yet captures experimental results surprisingly well [134]. By considering the tissue as a set of stretched cells represented by straight lines with a fixed length that span a curved substrate, the evolution of the tissue front can be visualized in a layer-by-layer fashion (Fig. 6e). This geometrical interpretation, while not explicitly modelling the formation of new tissue, is supported by the frequent observations of aligned actin filaments in pore channels and cells spanning concave spherical ($K > 0$, $H < 0$) substrates [69,130,134].

One aspect that is often not explicitly considered in these tissue growth models is the change in fluid flow properties that occurs as tissue progresses and fills the scaffold structure, potentially lowering the permeability and inhibiting the transport of oxygen and nutrients. Some models, however, consider the flow-induced shear stress in addition to the effects of substrate curvature [177,178]. This could be useful to quantitatively match the tissue growth predictions to *in vitro* experiments performed in a perfusion bioreactor [177]. Moreover, such models could assist in determining how to optimize scaffolds for tissue regeneration that balance curvature cues with a sufficient level of permeability [178]. In conclusion, it should be clear that relatively simple tissue growth laws, often based on some phenomenological applications of the curvature flow, perform remarkably well in predicting the shape and kinetics of tissue growth observed *in vitro*, and even *in vivo* [132]. It is, therefore, expected that such models will play ever more prominent roles in the scaffold design, especially when more of the underlying curvature guidance mechanisms are elucidated.

6. Discussion

We have reviewed the experimental evidence demonstrating that both individual cells and multicellular tissue constructs respond to the curvature of the underlying substrate, and have highlighted the dedicated theoretical models that aim to simulate this phenomenon. By emphasizing the notions of mean and Gaussian curvature, which are well-defined concepts from differential geometry, we hope to provide a more formal framework to describe cell- and tissue-level curvature guidance, with the ultimate aim of better understanding geometry-driven tissue regeneration. While many of the underlying mechanisms are still not understood, it is clear that mesoscale substrate curvature should be considered as an important cue for directing the organization and kinetics of cells and tissues. The experimental and theoretical results that we have reviewed provide some general insights into curvature guidance at the cell and tissue levels, the most important of which are summarized below.

First, cells with pronounced stress fibers (*e.g.*, fibroblasts) seem to avoid curvature whenever possible. On cylindrical substrates, such cells align in the longitudinal direction (*i.e.*, the direction of zero curvature). On the concave side of spherical substrates, where curvature is omnipresent, cells have the option to span the substrate to avoid being curved. Even on saddle shapes, which are convex in one direction and concave in the other, cells could span the concave part to avoid curvature as much as possible. As such, one might use the term curvature-avoidance rather than curvature guidance [61].

Second, both individually operating cells and multicellular ECM-rich tissue seem to favor concavities ($H < 0$) over convexities ($H > 0$). This observation holds for cylindrical-like ($K = 0$) as well as spherical-like ($K > 0$) substrates. Individual cells seem to favor migration towards concavities and avoid convex spherical caps, unless they are shallow. Osteoid-like tissue grows faster in concavities with higher curvature, and hardly shows any growth on convex regions, until the moment when the local curvature becomes concave due to tissue progression.

Third, tensile forces form the foundation of curvature guidance at both the single-cell and tissue-level scales. At the cell level, actomyosin contractility in conjunction with substrate geometry gives rise to a net normal force that either relieves or compresses the nucleus, thereby enabling individual cells to sense and respond to mesoscale curvature. The collective organization of cells in osteoid-like tissue results in a surface tension, causing the developing tissue to exhibit a viscous fluid-like behavior that evolves towards seemingly energy-minimizing configurations.

Finally, surfaces with negative Gaussian curvature (*i.e.*, saddle shapes) are largely unexplored in the current cell-response and tissue-growth studies, despite bearing high physiological relevance. Most research has been performed using either developable or spherical geometries, and the focus has been on either line curvature (*i.e.*, the curvature of pore cross sections), or on the mean curvature. The geometries that cells encounter *in vivo* are generally more complex, exhibiting wide variations of both mean and Gaussian curvatures, rendering purely spherical and intrinsically flat shapes rather the exception than the rule. For example, saddle shapes will emerge wherever branching and bending of tubular structures occurs, such as in blood vessels or the respiratory system. Additionally, every outwards-bulging spherical pouch, cyst, or vessel-like structure attached to a relatively flat tissue layer will exhibit negative Gaussian curvature at the neck region (the transition between the flat substrate and the spherical bulge). Moreover, complex network topologies, such as those found in trabecular bone, are known to be hyperbolic (saddle-shaped) on average. As such, it is essential to include substrates with negative Gaussian curvature within the spectrum of future curvature guidance studies.

Despite such general observations, it is important to emphasize that different cell types could be expected to behave differently to substrate curvature. For example, epithelial cells and fibroblasts align differently on cylindrical substrates, attributed to a change in the elastic energy balance [59,92]. Moreover, the curvature magnitudes that can be sensed by cells depend on the cell size. For example, MSCs might respond to certain curvature magnitudes while macrophages do not, possibly because of the smaller sizes of the latter [52]. Nonetheless, it is safe to state that substrate curvatures with the appropriate magnitude present an important cue to various types of adherent cells, and that the response of those cells can be understood from a mechanics-based perspective. Regarding tissue growth, most research has focused on osteoid-like tissue, with the ultimate aim of understanding scaffold geometry-guided tissue regeneration. Despite consistent experimental observations and promising predictions with theoretical models, a more mechanistic understanding of tissue evolution in response to curvature would be desirable. In this respect, it would be of interest to better link the insights made at the level of individual cells to the tissue scale, to understand how the response of single cells eventually gives rise to emergent tissue organization.

6.1. The implications for porous scaffold design

Within the field of tissue engineering, porous scaffolds are increasingly being considered for the active guidance and stimulation of the tissue regeneration process [154]. The rapid advances in additive manufacturing have resulted in an unprecedented freedom and control in the design of 3D porous scaffolds [179]. As such, the curvature of these scaffolds could be optimized to meet the various criteria that are relevant for tissue engineering applications including the mechanical, mass transfer, and biological properties. For example, scaffold curvatures could be optimized to provide a high initial tissue growth rate, yet maintain a desirable level of permeability [131,170], an endeavor that significantly benefits from efficient *in silico* models that consider both criteria [177]. The majority of the research into geometrical scaffold

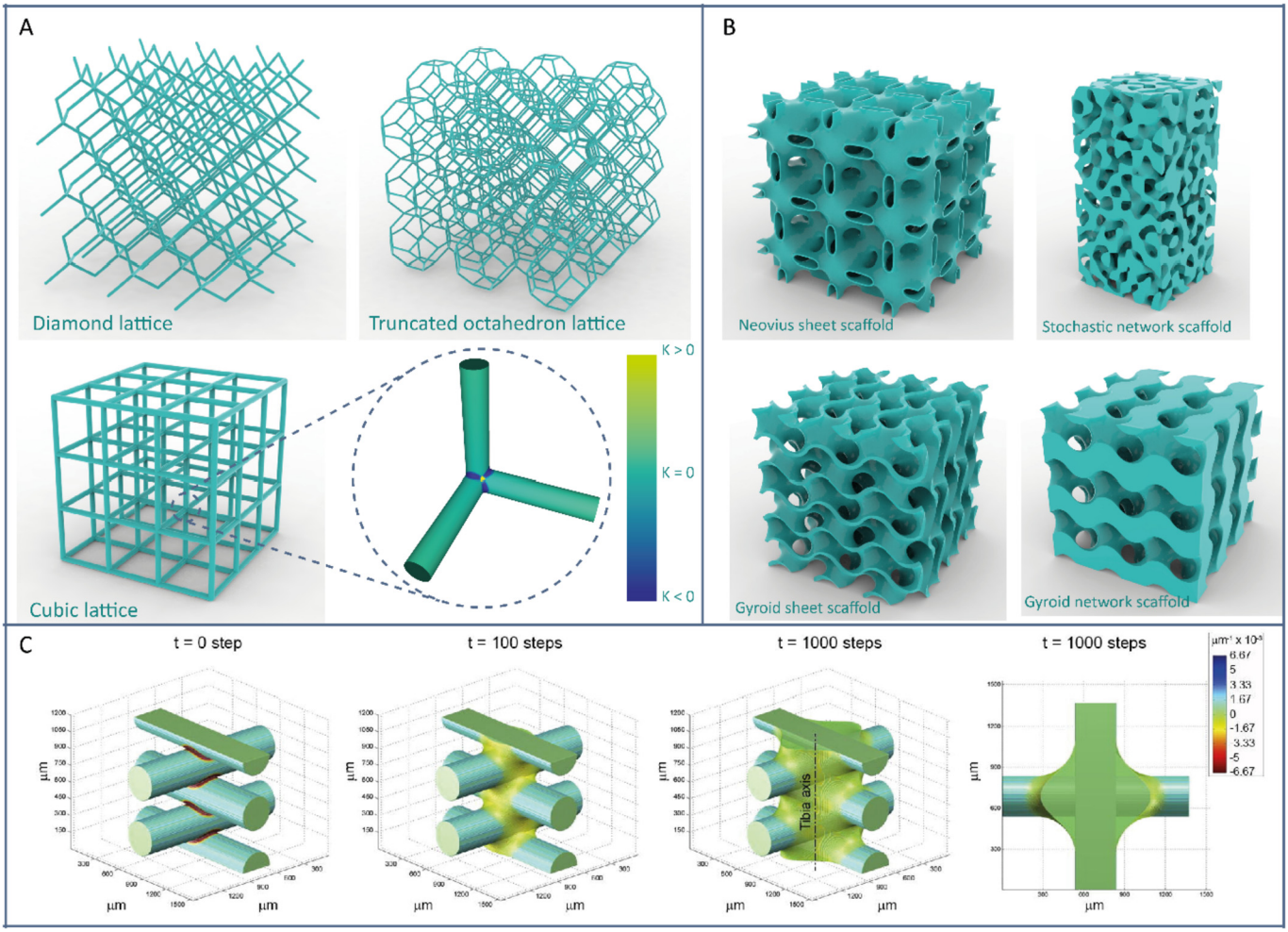

Fig. 7. 3D porous scaffolds for bone tissue regeneration. a) Some examples of strut-based scaffolds: the diamond lattice (top left), the truncated octahedron lattice (top right), and the cubic lattice (bottom left). Lattice structures with cylindrical struts exhibit non-zero Gaussian curvatures at the locations of the strut connections. b) Some examples of sheet-based scaffold designs: a Neovius sheet-scaffold (top left), a stochastic network-scaffold obtained with Gaussian random fields (top right), a Gyroid sheet-scaffold (bottom left), and a Gyroid network-scaffold (bottom right). The Neovius and Gyroid scaffolds are examples of scaffolds based on TPMS. c) Curvature-driven tissue growth predictions on the 0/90° scaffold used *in vivo* by Paris et al. [132]. Tissue starts growing from the strut intersections. Obtained with permission from Elsevier.

design and the effects of scaffold geometry on cell and tissue response has been directed at bone scaffolds, used in the treatment of segmental bone defects [180]. This is partly because bone itself is characterized by a highly complex, porous geometry, making it only natural that geometrical cues are considered in the design of synthetic bone substitutes [154]. Moreover, the developments in additively manufactured bone scaffolds build upon several decades of research into orthopedic implants, making this type of tissue scaffolds one of the most widely studied. As such, we will focus on bone scaffolds in this section, but we emphasize that the same principle of involving curvature in the design process could be applied to the other types of tissue scaffolds as well.

Although a myriad of 3D scaffold designs could be generated, such designs can roughly be classified in two major categories: 1. strut-based, network-like scaffolds and 2. sheet-based, foam-like scaffolds, both of which could be periodic or irregular [181]. The former has been widely considered for bone tissue applications, and could, for example, be derived from space-filling tessellations of polyhedra or well-known crystallographic arrangements (Fig. 7a). Sheet-based scaffolds exhibit more complex, smooth morphologies that could, for example, be designed using numerically simulated spinodal decomposition (Fig. 7b) [182,183]. From a curvature perspective, the sheet-based morphologies offer a richer design space, whereby large variations in both mean and Gaussian curvatures throughout the scaffold are possible. The strut-based scaffolds, however, offer a much smaller and more discrete curvature spectrum. For example, typical scaffolds with cylindrical struts exhibit zero Gaussian curvature and constant (positive) mean curvature on the strut surface, and only show concave regions with higher mean curvatures and non-zero Gaussian curvatures at the strut intersections (Fig. 7a). Given the experimental evidence showing very limited tissue growth on convex regions, it could be argued that cylindrical-strut based scaffolds are not very efficient from a curvature-guided tissue growth perspective. Indeed, *in vivo* and *in silico* results have confirmed that tissue growth initiates from the strut intersections in a simple strut-based scaffold (Fig. 7c) [132]. It, therefore, seems desirable to tune the mean and Gaussian curvatures of a scaffold in such a way to favor fast tissue regeneration. However, there are geometrical restrictions to the possible combinations of the mean and Gaussian curvatures, making it impossible to tune them independently or to fully decouple them from the global scaffold topology. For example, constant positive Gaussian curvature can only be achieved on the surface of a sphere, while a surface with constant negative Gaussian curvature can even not be realized in 3D Euclidean space according to Hilbert's theorem [21]. Moreover, curvature is scale-dependent, which means that a change in the curvature must be accompanied by a change in size. However, it is primarily the connection between surface curvature and global topology that places constraints on the ability to tune curvature

distributions throughout a scaffold. As mentioned in Section 2.1, the Gauss-Bonnet theorem dictates that the area-integrated Gaussian curvature of a surface is proportional to the genus (number of "handles") of that surface. More specifically, surfaces with $g > 1$ will be, in an integral sense, saddle-shaped or hyperbolic. The intricate network- or foam-like topologies of strut- and sheet-based scaffolds have $g \gg 1$, which means that they must contain regions with $K < 0$ to satisfy the Gauss-Bonnet theorem. Even the strut-based scaffolds, in which most of the area has $K = 0$ (on the strut surfaces), must contain saddle-shaped regions to balance the integral Gaussian curvature. Indeed, saddle-shaped regions are found at the intersections. The inherent hyperbolic nature of 3D porous scaffolds calls for a deeper investigation into the effects of negative Gaussian curvature on cells and tissues, yet very few studies have employed saddle-shaped substrates in single cell and tissue growth studies so far. Nonetheless, a particular class of saddle-shaped sheet-like morphologies, namely triply periodic minimal surfaces (TPMS), has recently started to receive widespread attention, in part due to the curvature arguments. TPMS are periodic, bicontinuous morphologies that locally minimize area and have $H = 0$ and $K \leq 0$ everywhere (Fig. 7b). It has been hypothesized that TPMS-based scaffolds could present "biomimetic" curvature cues, due to the similar mean curvature profile that has been observed in trabecular bone [172,184,185]. However, it remains unclear whether regular TPMS or their variations could, indeed, constitute optimal "curvature-guiding" scaffolds. In this regard, it could be questioned whether designing scaffolds based on the structure of healthy bone (*i.e.*, the homeostatic "end-state"), is an effective strategy towards fast regeneration of new tissue [186].

6.2. Opportunities for 4D printing

While 3D printing enables the fabrication of a wealth of complex porous geometries, emerging 4D printing technologies have recently started to receive considerable interest too. 4D printing adds time as another dimension to conventional 3D printing, resulting in structures that can change shape over time, typically by employing stimuli-responsive materials [187–189]. Since inception, 4D printing (or shape-shifting in general) has been considered as a novel platform for biomedical applications [190–192], opening new avenues towards encapsulation [84,193], biomedical devices [194,195], shape-changing scaffolds [196,197], or 2D-to-3D fabrication of cellular solids [198,199]. In the light of the curvature guidance principles discussed here, shape-shifting could enable temporal control over the geometrical environment of cells and tissues, in order to guide their evolution. For example, stimuli-responsive materials can be used to develop shape-changing substrates that allow for dynamic spatio-temporal control over the single-cell environment [200]. This might, for example, be useful to endow stem cells with a history of curvature cues that could affect their fate, as the lineage commitment of stem cells has been shown to be influenced by their past physical environments [201,202]. Furthermore, precisely patterning mesenchymal stromal cells in a collagenous ECM gel enables spontaneous *in vitro* tissue shape-shifting, reminiscent of the complex shape formation observed during *in vivo* development [203]. While 4D printing for tissue engineering is still in its infancy, it is expected that the ability to change the local geometry (*i.e.*, curvature) of the cellular environment with time could offer novel pathways to enhance the guiding and stimulating functions of tissue scaffolds.

6.3. Outlook

We already mentioned that a limited number of different substrate geometries has been employed in many single cell studies, often involving cylindrical or spherical shapes. This could, in part, be explained by the challenges associated with the microfabrication of cell-scale substrates. For example, most early studies resorted to cylindrical wires [54,58–60] to present the cells with a curved environment. However, rapid advances in microfabrication techniques, including micromachining [52,204], soft lithography [205,206], and two-photon polymerization [207,208] are enabling the robust fabrication of curved cellular environments with unprecedented design freedom [209]. Consequently, these technologies are expected to facilitate more in-depth studies of cell response to the various types of substrate curvatures. For example, they could allow for the investigation of cell response to developable surfaces other than cylinders (*e.g.*, cones or tangent developables), which also have zero Gaussian and non-zero mean curvature. Given the observed behavior on cylinders, it is expected that cells align in the zero-curvature direction on all types of developable surfaces. In addition to those specific types of substrates, curvature guidance studies could in general benefit from a broader spectrum of curved substrates, such as symmetric and non-symmetric saddles, ellipsoidal shapes, and other curvature landscapes with variations in mean and Gaussian curvatures. The same rationale at a larger scale applies to the tissue level, where additively manufactured scaffolds with precise curvature fields would be useful tools for investigating the curvature-guided tissue growth. In this regard, sheet-based scaffolds with controllable curvature profiles (*e.g.*, structures based on triply periodic constant mean curvature surfaces [210]), hold the most promise.

7. Conclusions

In conclusion, we reviewed the recent evidence that demonstrates the role of mesoscale substrate curvature on cell and tissue responses. By invoking the formal curvature descriptions provided by differential geometry (*i.e.*, mean and Gaussian surface curvatures), we hope to equip the reader with a more univocal framework to describe cell and tissue-level curvature guidance. We highlighted that much of the emergent organization and dynamics in response to substrate curvature could be explained from a mechanics perspective, involving actomyosin contractility on the cell level and surface tension on the tissue level. Moreover, experimental observations of tissue growth on 3D scaffolds can be replicated surprisingly well using phenomenological growth models that are reminiscent of the mathematical concept of curvature flow. While the underlying mechanisms are not yet fully uncovered and experimental evidence involving a broader curvature spectrum is necessary, the experimental and computational insights that we have reviewed show that substrate curvature should, indeed, be considered as an important cue in regulating cell response and guiding tissue growth. These curvature guidance principles could have far-reaching implications not only in understanding morphogenesis, defect healing, and bone remodeling, but also in the design of tissue engineering scaffolds and regenerative medicine therapies.

Acknowledgments

This research has received funding from the European Research Council under the ERC grant agreement n° [677575].

References

[1] B.D. Wilts, P.L. Clode, N.H. Patel, G.E. Schröder-Turk, Nature's functional nanomaterials: growth or self-assembly? MRS Bull. 44 (2) (2019) 106–112.
[2] J.R. Weeks, The Shape of Space, CRC press, Boca Raton, FL, USA, 2001.
[3] D.A.W. Thompson, On Growth and Form, Cambridge University Press, Cambridge, 1992.
[4] T. Iskratsch, H. Wolfenson, M.P. Sheetz, Appreciating force and shape—the rise of mechanotransduction in cell biology, Nat. Rev. Mol. Cell Biol. 15 (12) (2014) 825.
[5] D.E. Discher, P. Janmey, Y.-l. Wang, Tissue cells feel and respond to the stiffness of their substrate, Science 310 (5751) (2005) 1139–1143.
[6] A.J. Engler, S. Sen, H.L. Sweeney, D.E. Discher, Matrix elasticity directs stem cell lineage specification, Cell 126 (4) (2006) 677–689.
[7] O. Chaudhuri, L. Gu, D. Klumpers, M. Darnell, S.A. Bencherif, J.C. Weaver, N. Huebsch, H.-p. Lee, E. Lippens, G.N. Duda, Hydrogels with tunable stress relaxation regulate stem cell fate and activity, Nat. Mater. 15 (3) (2016) 326.

[8] X. Trepat, L. Deng, S.S. An, D. Navajas, D.J. Tschumperlin, W.T. Gerthoffer, J.P. Butler, J.J. Fredberg, Universal physical responses to stretch in the living cell, Nature 447 (7144) (2007) 592.
[9] A. Livne, E. Bouchbinder, B. Geiger, Cell reorientation under cyclic stretching, Nat. Commun. 5 (2014) 3938.
[10] V. Vogel, M. Sheetz, Local force and geometry sensing regulate cell functions, Nat. Rev. Mol. Cell Biol. 7 (4) (2006) 265.
[11] J. Eyckmans, T. Boudou, X. Yu, C.S. Chen, A hitchhiker's guide to mechanobiology, Dev. Cell 21 (1) (2011) 35–47.
[12] K.A. Jansen, D.M. Donato, H.E. Balcioglu, T. Schmidt, E.H. Danen, G.H. Koenderink, A guide to mechanobiology: where biology and physics meet, Biochim. Biophys. Acta Mol. Cell Res. 1853 (11) (2015) 3043–3052.
[13] N. Wang, J.D. Tytell, D.E. Ingber, Mechanotransduction at a distance: mechanically coupling the extracellular matrix with the nucleus, Nat. Rev. Mol. Cell Biol. 10 (1) (2009) 75.
[14] Y. Li, Y. Xiao, C. Liu, The horizon of materiobiology: a perspective on material-guided cell behaviors and tissue engineering, Chem. Rev. 117 (5) (2017) 4376–4421.
[15] M.J. Dalby, N. Gadegaard, R.O. Oreffo, Harnessing nanotopography and integrin–matrix interactions to influence stem cell fate, Nat. Mater. 13 (6) (2014) 558.
[16] L.E. McNamara, R.J. McMurray, M.J. Biggs, F. Kantawong, R.O. Oreffo, M.J. Dalby, Nanotopographical control of stem cell differentiation, J. Tissue Eng. 2010 (2010) 120623.
[17] S. Dobbenga, L.E. Fratila-Apachitei, A.A. Zadpoor, Nanopattern-induced osteogenic differentiation of stem cells - a systematic review, Acta Biomater. 46 (2016) 3–14.
[18] K. Modaresifar, S. Azizian, M. Ganjian, L.E. Fratila-Apachitei, A.A. Zadpoor, Bactericidal effects of nanopatterns: a systematic review, Acta Biomater. 83 (2018) 29–36.
[19] P. Kollmannsberger, C.M. Bidan, J.W.C. Dunlop, P. Fratzl, The physics of tissue patterning and extracellular matrix organisation: how cells join forces, Soft Matter 7 (20) (2011).
[20] S. Hyde, Z. Blum, T. Landh, S. Lidin, B.W. Ninham, S. Andersson, K. Larsson, The Language of Shape: the Role of Curvature in Condensed Matter: Physics, Chemistry and Biology, Elsevier Science, Amsterdam, The Netherlands, 1996.
[21] D. Hilbert, S. Cohn-Vossen, Geometry and the Imagination, Chelsea Publishing Company, New York, USA, 1990.
[22] S.J.P. Callens, A.A. Zadpoor, From flat sheets to curved geometries: origami and kirigami approaches, Mater. Today 21 (3) (2018) 241–264.
[23] C.M. Nelson, M.M. VanDuijn, J.L. Inman, D.A. Fletcher, M.J. Bissell, Tissue geometry determines sites of mammary branching morphogenesis in organotypic cultures, Science 314 (5797) (2006) 298–300.
[24] H.A. Messal, S. Alt, R.M. Ferreira, C. Gribben, V.M.-Y. Wang, C.G. Cotoi, G. Salbreux, A. Behrens, Tissue curvature and apicobasal mechanical tension imbalance instruct cancer morphogenesis, Nature 566 (7742) (2019) 126.
[25] J. Zimmerberg, M.M. Kozlov, How proteins produce cellular membrane curvature, Nat. Rev. Mol. Cell Biol. 7 (1) (2006) 9.
[26] R. Parthasarathy, J.T. Groves, Curvature and spatial organization in biological membranes, Soft Matter 3 (1) (2006) 24–33.
[27] M.E. Evans, G.E. Schröder-Turk, In a material world hyperbolic geometry in biological materials, Asia Pac. Math. Newsl. 5 (2) (2015) 21–30.
[28] Z.A. Almsherqi, T. Landh, S.D. Kohlwein, Y. Deng, Cubic membranes: the missing dimension of cell membrane organization, Int. Rev. Cel. Mol. Bio. 274 (2009) 275–342.
[29] Y. Deng, M. Mieczkowski, Three-dimensional periodic cubic membrane structure in the mitochondria of amoebaeChaos carolinensis, Protoplasma 203 (1–2) (1998) 16–25.
[30] N.D. Bade, T. Xu, R.D. Kamien, R.K. Assoian, K.J. Stebe, Gaussian curvature directs stress fiber orientation and cell migration, Biophys. J. 114 (6) (2018) 1467–1476.
[31] C.M. Nelson, On buckling morphogenesis, J. Biomech. Eng. 138 (2) (2016) 021005.
[32] D.P. Richman, R.M. Stewart, J.W. Hutchinson, V.S. Caviness, Mechanical model of brain convolutional development, Science 189 (4196) (1975) 18–21.
[33] A.E. Shyer, T. Tallinen, N.L. Nerurkar, Z. Wei, E.S. Gil, D.L. Kaplan, C.J. Tabin, L. Mahadevan, Villification: how the gut gets its villi, Science 342 (6155) (2013) 212–218.
[34] H.Y. Kim, M.-F. Pang, V.D. Varner, L. Kojima, E. Miller, D.C. Radisky, C.M. Nelson, Localized smooth muscle differentiation is essential for epithelial bifurcation during branching morphogenesis of the mammalian lung, Dev. Cell 34 (6) (2015) 719–726.
[35] H. Takigawa-Imamura, R. Morita, T. Iwaki, T. Tsuji, K. Yoshikawa, Tooth germ invagination from cell–cell interaction: working hypothesis on mechanical instability, J. Theor. Biol. 382 (2015) 284–291.
[36] S.P. Timoshenko, S. Woinowsky-Krieger, Theory of Plates and Shells, McGraw-hill, 1959.
[37] C.M. Nelson, R.P. Jean, J.L. Tan, W.F. Liu, N.J. Sniadecki, A.A. Spector, C.S. Chen, Emergent patterns of growth controlled by multicellular form and mechanics, Proc. Natl. Acad. Sci. 102 (33) (2005) 11594–11599.
[38] D.E. Ingber, Mechanical control of tissue growth: function follows form, Proc. Natl. Acad. Sci. 102 (33) (2005) 11571–11572.
[39] N. Stollman, J.B. Raskin, Diverticular disease of the colon, The Lancet 363 (9409) (2004) 631–639.
[40] P.D. Wilson, Polycystic kidney disease, N. Engl. J. Med. 350 (2) (2004) 151–164.
[41] J. Lee, A.A. Abdeen, K.L. Wycislo, T.M. Fan, K.A. Kilian, Interfacial geometry dictates cancer cell tumorigenicity, Nat. Mater. 15 (8) (2016) 856.
[42] H. Jinnai, H. Watashiba, T. Kajihara, Y. Nishikawa, M. Takahashi, M. Ito, Surface curvatures of trabecular bone microarchitecture, Bone 30 (1) (2002) 191–194.
[43] H. Jinnai, Y. Nishikawa, M. Ito, S.D. Smith, D.A. Agard, R.J. Spontak, Topological similarity of sponge-like bicontinuous morphologies differing in length scale, Adv. Mater. 14 (22) (2002) 1615–1618.
[44] T.L. Downing, J. Soto, C. Morez, T. Houssin, A. Fritz, F. Yuan, J. Chu, S. Patel, D.V. Schaffer, S. Li, Biophysical regulation of epigenetic state and cell reprogramming, Nat. Mater. 12 (12) (2013) 1154.
[45] A. Mathur, S.W. Moore, M.P. Sheetz, J. Hone, The role of feature curvature in contact guidance, Acta Biomater. 8 (7) (2012) 2595–2601.
[46] M. Simunovic, G.A. Voth, A. Callan-Jones, P. Bassereau, When physics takes over: BAR proteins and membrane curvature, Trends Cell Biol. 25 (12) (2015) 780–792.
[47] C. Mim, V.M. Unger, Membrane curvature and its generation by BAR proteins, Trends Biochem. Sci. 37 (12) (2012) 526–533.
[48] B.J. Peter, H.M. Kent, I.G. Mills, Y. Vallis, P.J.G. Butler, P.R. Evans, H.T. McMahon, BAR domains as sensors of membrane curvature: the amphiphysin BAR structure, Science 303 (5657) (2004) 495–499.
[49] A.J. Patel, M. Lazdunski, E. Honoré, Lipid and mechano-gated 2P domain K+ channels, Curr. Opin. Cell Biol. 13 (4) (2001) 422–428.
[50] W. Zhao, L. Hanson, H.-Y. Lou, M. Akamatsu, P.D. Chowdary, F. Santoro, J.R. Marks, A. Grassart, D.G. Drubin, Y. Cui, Nanoscale manipulation of membrane curvature for probing endocytosis in live cells, Nat. Nanotechnol. 12 (8) (2017) 750.
[51] H.T. McMahon, J.L. Gallop, Membrane curvature and mechanisms of dynamic cell membrane remodelling, Nature 438 (7068) (2005) 590.
[52] L. Pieuchot, J. Marteau, A. Guignandon, T. Dos Santos, I. Brigaud, P.-F. Chauvy, T. Cloatre, A. Ponche, T. Petithory, P. Rougerie, M. Vassaux, J.-L. Milan, N.T. Wakhloo, A. Spangenberg, M. Bigerelle, K. Anselme, Curvotaxis directs cell migration through cell-scale curvature landscapes, Nat. Commun. 9 (1) (2018) 3995.
[53] P. Weiss, Experiments on cell and axon orientation in vitro: the role of colloidal exudates in tissue organization, J. Exp. Zool. 100 (3) (1945) 353–386.
[54] G. Dunn, J. Heath, A new hypothesis of contact guidance in tissue cells, Exp. Cell Res. 101 (1) (1976) 1–14.
[55] U.S. Schwarz, I.B. Bischofs, Physical determinants of cell organization in soft media, Med. Eng. Phys. 27 (9) (2005) 763–772.
[56] D. Baptista, L. Teixeira, C. van Blitterswijk, S. Giselbrecht, R. Truckenmüller, Overlooked? Underestimated? Effects of substrate curvature on cell behavior, Trends Biotechnol. 37 (8) (2019) 838–854.
[57] N.D. Bade, R.D. Kamien, R.K. Assoian, K.J. Stebe, Curvature and Rho activation differentially control the alignment of cells and stress fibers, Sci. Adv. 3 (9) (2017) e1700150.
[58] T.M. Svitkina, Y.A. Rovensky, A.D. Bershadsky, J.M. Vasiliev, Transverse pattern of microfilament bundles induced in epitheliocytes by cylindrical substrata, J. Cell Sci. 108 (2) (1995) 735–745.
[59] Y. Rovensky, V. Samoilov, Morphogenetic response of cultured normal and transformed fibroblasts, and epitheliocytes, to a cylindrical substratum surface. Possible role for the actin filament bundle pattern, J. Cell Sci. 107 (5) (1994) 1255–1263.
[60] E.M. Levina, L.V. Domnina, Y.A. Rovensky, J.M. Vasiliev, Cylindrical substratum induces different patterns of actin microfilament bundles in nontransformed and in ras-transformed epitheliocytes, Exp. Cell Res. 229 (1) (1996) 159–165.
[61] M. Werner, N.A. Kurniawan, G. Korus, C.V. Bouten, A. Petersen, Mesoscale substrate curvature overrules nanoscale contact guidance to direct bone marrow stromal cell migration, J. R. Soc. Interface 15 (145) (2018) 20180162.
[62] A.K. Yip, P. Huang, K.H. Chiam, Cell-cell adhesion and cortical actin bending govern cell elongation on negatively curved substrates, Biophys. J. 114 (7) (2018) 1707–1717.
[63] M. Werner, A. Petersen, N.A. Kurniawan, C.V. Bouten, Cell-perceived substrate curvature dynamically coordinates the direction, speed, and persistence of stromal cell migration, Adv. Biosyst. (2019) 1900080.
[64] M. Pilia, T. Guda, S.M. Shiels, M.R. Appleford, Influence of substrate curvature on osteoblast orientation and extracellular matrix deposition, J. Biol. Eng. 7 (1) (2013) 23.
[65] V. Hosseini, P. Kollmannsberger, S. Ahadian, S. Ostrovidov, H. Kaji, V. Vogel, A. Khademhosseini, Fiber-assisted molding (FAM) of surfaces with tunable curvature to guide cell alignment and complex tissue architecture, Small 10 (23) (2014) 4851–4857.
[66] K.H. Song, S.J. Park, D.S. Kim, J. Doh, Sinusoidal wavy surfaces for curvature-guided migration of T lymphocytes, Biomaterials 51 (2015) 151–160.
[67] S.J. Lee, S. Yang, Substrate curvature restricts spreading and induces differentiation of human mesenchymal stem cells, Biotechnol. J. 12 (9) (2017) 1700360.
[68] V. Malheiro, F. Lehner, V. Dinca, P. Hoffmann, K. Maniura-Weber, Convex and concave micro-structured silicone controls the shape, but not the polarization state of human macrophages, Biomater. Sci. 4 (11) (2016) 1562–1573.
[69] M. Werner, S.B. Blanquer, S.P. Haimi, G. Korus, J.W. Dunlop, G.N. Duda, D.W. Grijpma, A. Petersen, Surface curvature differentially regulates stem cell migration and differentiation via altered attachment morphology and nuclear deformation, Adv. Sci. 4 (2) (2017) 1600347.
[70] J.Y. Park, D.H. Lee, E.J. Lee, S.-H. Lee, Study of cellular behaviors on concave and convex microstructures fabricated from elastic PDMS membranes, Lab Chip 9 (14) (2009) 2043–2049.
[71] S. Van Helvert, C. Storm, P. Friedl, Mechanoreciprocity in cell migration, Nat. Cell Biol. 20 (1) (2018) 8.
[72] A.J. Ridley, M.A. Schwartz, K. Burridge, R.A. Firtel, M.H. Ginsberg, G. Borisy, J.T. Parsons, A.R. Horwitz, Cell migration: integrating signals from front to back,

Science 302 (5651) (2003) 1704–1709.
[73] R. Mayor, S. Etienne-Manneville, The front and rear of collective cell migration, Nat. Rev. Mol. Cell Biol. 17 (2) (2016) 97.
[74] S. Etienne-Manneville, A. Hall, Rho GTPases in cell biology, Nature 420 (6916) (2002) 629.
[75] M.D. Welch, R.D. Mullins, Cellular control of actin nucleation, Annu. Rev. Cell Dev. Biol. 18 (1) (2002) 247–288.
[76] D.A. Lauffenburger, A.F. Horwitz, Cell migration: a physically integrated molecular process, Cell 84 (3) (1996) 359–369.
[77] S.J. Lee, S. Yang, Micro glass ball embedded gels to study cell mechanobiological responses to substrate curvatures, Rev. Sci. Instrum. 83 (9) (2012) 094302.
[78] C. Hwang, Y. Park, J. Park, K. Lee, K. Sun, A. Khademhosseini, S.H. Lee, Controlled cellular orientation on PLGA microfibers with defined diameters, Biomed. Microdevices 11 (4) (2009) 739–746.
[79] J.R. Soiné, N. Hersch, G. Dreissen, N. Hampe, B. Hoffmann, R. Merkel, U.S. Schwarz, Measuring cellular traction forces on non-planar substrates, Interface Focus 6 (5) (2016) 20160024.
[80] H.G. Yevick, G. Duclos, I. Bonnet, P. Silberzan, Architecture and migration of an epithelium on a cylindrical wire, Proc. Natl. Acad. Sci. 112 (19) (2015) 5944–5949.
[81] R.M. Gouveia, E. Koudouna, J. Jester, F. Figueiredo, C.J. Connon, Template curvature influences cell alignment to create improved human corneal tissue equivalents, Adv. Biosyst. 1 (2017) 1700135.
[82] M. Murrell, P.W. Oakes, M. Lenz, M.L. Gardel, Forcing cells into shape: the mechanics of actomyosin contractility, Nat. Rev. Mol. Cell Biol. 16 (8) (2015) 486.
[83] A.K. Harris, P. Wild, D. Stopak, Silicone rubber substrata: a new wrinkle in the study of cell locomotion, Science 208 (4440) (1980) 177–179.
[84] K. Kuribayashi-Shigetomi, H. Onoe, S. Takeuchi, Cell origami: self-folding of three-dimensional cell-laden microstructures driven by cell traction force, PLoS One 7 (12) (2012) e51085.
[85] N.Q. Balaban, U.S. Schwarz, D. Riveline, P. Goichberg, G. Tzur, I. Sabanay, D. Mahalu, S. Safran, A. Bershadsky, L. Addadi, Force and focal adhesion assembly: a close relationship studied using elastic micropatterned substrates, Nat. Cell Biol. 3 (5) (2001) 466.
[86] S. Tadokoro, S.J. Shattil, K. Eto, V. Tai, R.C. Liddington, J.M. de Pereda, M.H. Ginsberg, D.A. Calderwood, Talin binding to integrin ß tails: a final common step in integrin activation, Science 302 (5642) (2003) 103–106.
[87] J.D. Humphries, P. Wang, C. Streuli, B. Geiger, M.J. Humphries, C. Ballestrem, Vinculin controls focal adhesion formation by direct interactions with talin and actin, J. Cell Biol. 179 (5) (2007) 1043–1057.
[88] K.A. DeMali, X. Sun, G.A. Bui, Force transmission at cell–cell and cell–matrix adhesions, Biochemistry 53 (49) (2014) 7706–7717.
[89] M. Vicente-Manzanares, X. Ma, R.S. Adelstein, A.R. Horwitz, Non-muscle myosin II takes centre stage in cell adhesion and migration, Nat. Rev. Mol. Cell Biol. 10 (11) (2009) 778.
[90] C.S. Rex, C.F. Gavin, M.D. Rubio, E.A. Kramar, L.Y. Chen, Y. Jia, R.L. Huganir, N. Muzyczka, C.M. Gall, C.A. Miller, Myosin IIb regulates actin dynamics during synaptic plasticity and memory formation, Neuron 67 (4) (2010) 603–617.
[91] S. Tojkander, G. Gateva, P. Lappalainen, Actin stress fibers–assembly, dynamics and biological roles, J. Cell Sci. 125 (8) (2012) 1855–1864.
[92] Y. Biton, S. Safran, The cellular response to curvature-induced stress, Phys. Biol. 6 (4) (2009) 046010.
[93] Y.-P. Lo, Y.-S. Liu, M.G. Rimando, J.H.-C. Ho, K.-h. Lin, O.K. Lee, Three-dimensional spherical spatial boundary conditions differentially regulate osteogenic differentiation of mesenchymal stromal cells, Sci. Rep. 6 (2016) 21253.
[94] M. Théry, A. Pépin, E. Dressaire, Y. Chen, M. Bornens, Cell distribution of stress fibres in response to the geometry of the adhesive environment, Cell motil, Cytoskel 63 (6) (2006) 341–355.
[95] A. Pathak, V.S. Deshpande, R.M. McMeeking, A.G. Evans, The simulation of stress fibre and focal adhesion development in cells on patterned substrates, J. R. Soc. Interface 5 (22) (2007) 507–524.
[96] A.J. Ridley, A. Hall, The small GTP-binding protein rho regulates the assembly of focal adhesions and actin stress fibers in response to growth factors, Cell 70 (3) (1992) 389–399.
[97] K.N. Dahl, A. Kalinowski, Nucleoskeleton mechanics at a glance, J. Cell Sci. 124 (5) (2011) 675–678.
[98] D.N. Simon, K.L. Wilson, The nucleoskeleton as a genome-associated dynamic 'network of networks', Nat. Rev. Mol. Cell Biol. 12 (11) (2011) 695.
[99] F. Guilak, J.R. Tedrow, R. Burgkart, Viscoelastic properties of the cell nucleus, Biochem. Biophys. Res. Commun. 269 (3) (2000) 781–786.
[100] J. Lammerding, Mechanics of the nucleus, Comp. Physiol. 1 (2) (2011) 783–807.
[101] C.H. Thomas, J.H. Collier, C.S. Sfeir, K.E. Healy, Engineering gene expression and protein synthesis by modulation of nuclear shape, Proc. Natl. Acad. Sci. 99 (4) (2002) 1972–1977.
[102] K.N. Dahl, A.J. Ribeiro, J. Lammerding, Nuclear shape, mechanics, and mechanotransduction, Circ. Res. 102 (11) (2008) 1307–1318.
[103] M. Crisp, Q. Liu, K. Roux, J. Rattner, C. Shanahan, B. Burke, P.D. Stahl, D. Hodzic, Coupling of the nucleus and cytoplasm: role of the LINC complex, J. Cell Biol. 172 (1) (2006) 41–53.
[104] K. Anselme, N.T. Wakhloo, P. Rougerie, L. Pieuchot, Role of the nucleus as a sensor of cell environment topography, Adv. Healthc. Mater. 7 (8) (2018) 1701154.
[105] S. Cho, J. Irianto, D.E. Discher, Mechanosensing by the nucleus: from pathways to scaling relationships, J. Cell Biol. 216 (2) (2017) 305–315.
[106] S.E. Szczesny, R.L. Mauck, The nuclear option: evidence implicating the cell nucleus in mechanotransduction, J. Biomech. Eng. 139 (2) (2017) 021006.
[107] S.B. Khatau, C.M. Hale, P. Stewart-Hutchinson, M.S. Patel, C.L. Stewart, P.C. Searson, D. Hodzic, D. Wirtz, A perinuclear actin cap regulates nuclear shape, Proc. Natl. Acad. Sci. 106 (45) (2009) 19017–19022.
[108] J. Lammerding, L.G. Fong, J.Y. Ji, K. Reue, C.L. Stewart, S.G. Young, R.T. Lee, Lamins A and C but not lamin B1 regulate nuclear mechanics, J. Biol. Chem. 281 (35) (2006) 25768–25780.
[109] R. McBeath, D.M. Pirone, C.M. Nelson, K. Bhadriraju, C.S. Chen, Cell shape, cytoskeletal tension, and RhoA regulate stem cell lineage commitment, Dev. Cell 6 (4) (2004) 483–495.
[110] J. Foolen, T. Yamashita, P. Kollmannsberger, Shaping tissues by balancing active forces and geometric constraints, J. Phys. D Appl. Phys. 49 (5) (2016).
[111] A. Katsumi, A.W. Orr, E. Tzima, M.A. Schwartz, Integrins in mechanotransduction, J. Biol. Chem. 279 (13) (2004) 12001–12004.
[112] D.E. Leckband, J. De Rooij, Cadherin adhesion and mechanotransduction, Annu. Rev. Cell Dev. Biol. 30 (2014) 291–315.
[113] A.R. Harris, L. Peter, J. Bellis, B. Baum, A.J. Kabla, G.T. Charras, Characterizing the mechanics of cultured cell monolayers, Proc. Natl. Acad. Sci. 109 (41) (2012) 16449–16454.
[114] W. Xi, T.B. Saw, D. Delacour, C.T. Lim, B. Ladoux, Material approaches to active tissue mechanics, Nat. Rev. Mater. (2018) 1.
[115] B. Lubarsky, M.A. Krasnow, Tube morphogenesis: making and shaping biological tubes, Cell 112 (1) (2003) 19–28.
[116] M. Ye, H.M. Sanchez, M. Hultz, Z. Yang, M. Bogorad, A.D. Wong, P.C. Searson, Brain microvascular endothelial cells resist elongation due to curvature and shear stress, Sci. Rep. 4 (2014) 4681.
[117] S.-M. Yu, J.M. Oh, J. Lee, W. Lee-Kwon, W. Jung, F. Amblard, S. Granick, Y.-K. Cho, Substrate curvature affects the shape, orientation, and polarization of renal epithelial cells, Acta Biomater. 77 (2018) 311–321.
[118] W. Xi, S. Sonam, T.B. Saw, B. Ladoux, C.T. Lim, Emergent patterns of collective cell migration under tubular confinement, Nat. Commun. 8 (1) (2017) 1517.
[119] M. Poujade, E. Grasland-Mongrain, A. Hertzog, J. Jouanneau, P. Chavrier, B. Ladoux, A. Buguin, P. Silberzan, Collective migration of an epithelial monolayer in response to a model wound, Proc. Natl. Acad. Sci. 104 (41) (2007) 15988–15993.
[120] B. Ladoux, R.-M. Mège, Mechanobiology of collective cell behaviours, Nat. Rev. Mol. Cell Biol. 18 (12) (2017) 743.
[121] J.P. Thiery, H. Acloque, R.Y. Huang, M.A. Nieto, Epithelial-mesenchymal transitions in development and disease, Cell 139 (5) (2009) 871–890.
[122] T. Yamashita, P. Kollmannsberger, K. Mawatari, T. Kitamori, V. Vogel, Cell sheet mechanics: how geometrical constraints induce the detachment of cell sheets from concave surfaces, Acta Biomater. 45 (2016) 85–97.
[123] F.A. Maechler, C. Allier, A. Roux, C. Tomba, Curvature dependent constraints drive remodeling of epithelia, J. Cell Sci. (2018) 222372jcs.
[124] G. Miquelard-Garnier, J.A. Zimberlin, C.B. Sikora, P. Wadsworth, A. Crosby, Polymer microlenses for quantifying cell sheet mechanics, Soft Matter 6 (2) (2010) 398–403.
[125] P. Gómez-Gálvez, P. Vicente-Munuera, A. Tagua, C. Forja, A.M. Castro, M. Letrán, A. Valencia-Expósito, C. Grima, M. Bermúdez-Gallardo, Ó. Serrano-Pérez-Higueras, Scutoids are a geometrical solution to three-dimensional packing of epithelia, Nat. Commun. 9 (1) (2018) 2960.
[126] C.M. Nelson, Epithelial packing: even the best of friends must part, Curr. Biol. 28 (20) (2018) R1197–R1200.
[127] E. Hannezo, J. Prost, J.-F. Joanny, Theory of epithelial sheet morphology in three dimensions, Proc. Natl. Acad. Sci. 111 (1) (2014) 27–32.
[128] J.K. Mouw, G. Ou, V.M. Weaver, Extracellular matrix assembly: a multiscale deconstruction, Nat. Rev. Mol. Cell Biol. 15 (12) (2014) 771.
[129] S. Ehrig, B. Schamberger, C. Bidan, A. West, C. Jacobi, K. Lam, P. Kollmannsberger, A. Petersen, P. Tomancak, K. Kommareddy, Surface tension determines tissue shape and growth kinetics, Sci. Adv. 5 (9) (2019) eaav9394.
[130] M. Rumpler, A. Woesz, J.W. Dunlop, J.T. van Dongen, P. Fratzl, The effect of geometry on three-dimensional tissue growth, J. R. Soc. Interface 5 (27) (2008) 1173–1180.
[131] C.M. Bidan, K.P. Kommareddy, M. Rumpler, P. Kollmannsberger, P. Fratzl, J.W. Dunlop, Geometry as a factor for tissue growth: towards shape optimization of tissue engineering scaffolds, Adv. Healthc. Mater. 2 (1) (2013) 186–194.
[132] M. Paris, A. Gotz, I. Hettrich, C.M. Bidan, J.W.C. Dunlop, H. Razi, I. Zizak, D.W. Hutmacher, P. Fratzl, G.N. Duda, W. Wagermaier, A. Cipitria, Scaffold curvature-mediated novel biomineralization process originates a continuous soft tissue-to-bone interface, Acta Biomater. 60 (2017) 64–80.
[133] J. Knychala, N. Bouropoulos, C. Catt, O. Katsamenis, C. Please, B. Sengers, Pore geometry regulates early stage human bone marrow cell tissue formation and organisation, Ann. Biomed. Eng. 41 (5) (2013) 917–930.
[134] C.M. Bidan, K.P. Kommareddy, M. Rumpler, P. Kollmannsberger, Y.J. Brechet, P. Fratzl, J.W. Dunlop, How linear tension converts to curvature: geometric control of bone tissue growth, PLoS One 7 (5) (2012) e36336.
[135] K.P. Kommareddy, C. Lange, M. Rumpler, J.W. Dunlop, I. Manjubala, J. Cui, K. Kratz, A. Lendlein, P. Fratzl, Two stages in three-dimensional in vitro growth of tissue generated by osteoblastlike cells, Biointerphases 5 (2) (2010) 45–52.
[136] J.R. Vetsch, R. Muller, S. Hofmann, The influence of curvature on three-dimensional mineralized matrix formation under static and perfused conditions: an in vitro bioreactor model, J. R. Soc. Interface 13 (123) (2016).
[137] E. Tamjid, A. Simchi, J.W. Dunlop, P. Fratzl, R. Bagheri, M. Vossoughi, Tissue growth into three-dimensional composite scaffolds with controlled micro-features and nanotopographical surfaces, J. Biomed. Mater. Res. A 101 (10) (2013) 2796–2807.
[138] C.M. Bidan, P. Kollmannsberger, V. Gering, S. Ehrig, P. Joly, A. Petersen, V. Vogel, P. Fratzl, J.W. Dunlop, Gradual conversion of cellular stress patterns into pre-

stressed matrix architecture during in vitro tissue growth, J. R. Soc. Interface 13 (118) (2016) 20160136.
[139] E. Gamsjager, C.M. Bidan, F.D. Fischer, P. Fratzl, J.W. Dunlop, Modelling the role of surface stress on the kinetics of tissue growth in confined geometries, Acta Biomater. 9 (3) (2013) 5531–5543.
[140] T. Hayashi, R.W. Carthew, Surface mechanics mediate pattern formation in the developing retina, Nature 431 (7009) (2004) 647.
[141] M.L. Manning, R.A. Foty, M.S. Steinberg, E.-M. Schoetz, Coaction of intercellular adhesion and cortical tension specifies tissue surface tension, Proc. Natl. Acad. Sci. 107 (28) (2010) 12517–12522.
[142] T. Lecuit, P.-F. Lenne, Cell surface mechanics and the control of cell shape, tissue patterns and morphogenesis, Nat. Rev. Mol. Cell Biol. 8 (8) (2007) 633.
[143] R.A. Foty, G. Forgacs, C.M. Pfleger, M.S. Steinberg, Liquid properties of embryonic tissues: measurement of interfacial tensions, Phys. Rev. Lett. 72 (14) (1994) 2298.
[144] J. Käfer, T. Hayashi, A.F. Marée, R.W. Carthew, F. Graner, Cell adhesion and cortex contractility determine cell patterning in the drosophilaretina, Proc. Natl. Acad. Sci. 104 (47) (2007) 18549–18554.
[145] P.S. Laplace, Traité de mécanique céleste, de l'Imprimerie de Crapelet, 1799.
[146] I.B. Bischofs, F. Klein, D. Lehnert, M. Bastmeyer, U.S. Schwarz, Filamentous network mechanics and active contractility determine cell and tissue shape, Biophys. J. 95 (7) (2008) 3488–3496.
[147] I.B. Bischofs, S.S. Schmidt, U.S. Schwarz, Effect of adhesion geometry and rigidity on cellular force distributions, Phys. Rev. Lett. 103 (4) (2009) 048101.
[148] P. Kollmannsberger, C.M. Bidan, J.W. Dunlop, P. Fratzl, V. Vogel, Tensile forces drive a reversible fibroblast-to-myofibroblast transition during tissue growth in engineered clefts, Sci. Adv. 4 (1) (2018) eaao4881.
[149] T.B. Saw, W. Xi, B. Ladoux, C.T. Lim, Biological tissues as active nematic liquid crystals, Adv. Mater. 30 (47) (2018) 1802579.
[150] A. Cipitria, C. Lange, H. Schell, W. Wagermaier, J.C. Reichert, D.W. Hutmacher, P. Fratzl, G.N. Duda, Porous scaffold architecture guides tissue formation, J. Bone Miner. Res. 27 (6) (2012) 1275–1288.
[151] A. Scarano, V. Perrotti, L. Artese, M. Degidi, D. Degidi, A. Piattelli, G. Iezzi, Blood vessels are concentrated within the implant surface concavities: a histologic study in rabbit tibia, Odontology 102 (2) (2014) 259–266.
[152] T.P. Wyatt, J. Fouchard, A. Lisica, N. Khalilgharibi, B. Baum, P. Recho, A.J. Kabla, G.T. Charras, Actomyosin controls planarity and folding of epithelia in response to compression, Nat. Mater. (2019) 1–9.
[153] L. Geris, T. Lambrechts, A. Carlier, I. Papantoniou, The future is digital: in silico tissue engineering, Curr. Opin. Biomed. Eng. 6 (2018) 92–98.
[154] A.A. Zadpoor, Bone tissue regeneration: the role of scaffold geometry, Biomater. Sci. 3 (2) (2015) 231–245.
[155] D. Ambrosi, G.A. Ateshian, E.M. Arruda, S. Cowin, J. Dumais, A. Goriely, G.A. Holzapfel, J.D. Humphrey, R. Kemkemer, E. Kuhl, Perspectives on biological growth and remodeling, J. Mech. Phys. Solids 59 (4) (2011) 863–883.
[156] V.S. Deshpande, R.M. McMeeking, A.G. Evans, A bio-chemo-mechanical model for cell contractility, Proc. Natl. Acad. Sci. 103 (38) (2006) 14015–14020.
[157] I.L. Novak, B.M. Slepchenko, A. Mogilner, L.M. Loew, Cooperativity between cell contractility and adhesion, Phys. Rev. Lett. 93 (26) (2004) 268109.
[158] G. Danuser, J. Allard, A. Mogilner, Mathematical modeling of eukaryotic cell migration: insights beyond experiments, Annu. Rev. Cell Dev. Biol. 29 (2013) 501–528.
[159] J.A. Sanz-Herrera, P. Moreo, J.M. García-Aznar, M. Doblaré, On the effect of substrate curvature on cell mechanics, Biomaterials 30 (34) (2009) 6674–6686.
[160] D.E. Ingber, Tensegrity: the architectural basis of cellular mechanotransduction, Annu. Rev. Physiol. 59 (1) (1997) 575–599.
[161] M. Vassaux, J. Milan, Stem cell mechanical behaviour modelling: substrate's curvature influence during adhesion, Biomechanics Model. Mechanobiol. 16 (4) (2017) 1295–1308.
[162] M. Jean, The non-smooth contact dynamics method, Comput. Methods Appl. Math. 177 (3–4) (1999) 235–257.
[163] X. He, Y. Jiang, Substrate curvature regulates cell migration, Phys. Biol. 14 (3) (2017) 035006.
[164] O.I. Frette, G. Virnovsky, D. Silin, Estimation of the curvature of an interface from a digital 2D image, Comput. Mater. Sci. 44 (3) (2009) 867–875.
[165] C. Epstein, M. Gage, The Curve Shortening Flow, Wave Motion: Theory, Modelling, and Computation, Springer, 1987, pp. 15–59.
[166] C.M. Bidan, F.M. Wang, J.W. Dunlop, A three-dimensional model for tissue deposition on complex surfaces, Comput. Method Biomech. 16 (10) (2013) 1056–1070.
[167] Y. Guyot, I. Papantoniou, Y.C. Chai, S. Van Bael, J. Schrooten, L. Geris, A computational model for cell/ECM growth on 3D surfaces using the level set method: a bone tissue engineering case study, Biomechanics Model. Mechanobiol. 13 (6) (2014) 1361–1371.
[168] J.A. Sethian, P. Smereka, Level set methods for fluid interfaces, Annu. Rev. Fluid Mech. 35 (1) (2003) 341–372.
[169] J.A. Sethian, Level Set Methods and Fast Marching Methods: Evolving Interfaces in Computational Geometry, Fluid Mechanics, Computer Vision, and Materials Science, Cambridge university press, 1999.
[170] P.F. Egan, K.A. Shea, S.J. Ferguson, Simulated tissue growth for 3D printed scaffolds, Biomechanics Model. Mechanobiol. 17 (2018) 1481–1495.
[171] K.A. Brakke, The Motion of a Surface by its Mean Curvature, Princeton University Press, 2015.
[172] S.C. Kapfer, S.T. Hyde, K. Mecke, C.H. Arns, G.E. Schröder-Turk, Minimal surface scaffold designs for tissue engineering, Biomaterials 32 (29) (2011) 6875–6882.
[173] S. Ehrig, C.M. Bidan, A. West, C. Jacobi, K. Lam, P. Kollmannsberger, A. Petersen, P. Tomancak, K. Kommareddy, F.D. Fischer, P. Fratzl, J.W.C. Dunlop, Surface Tension Determines Tissue Shape and Growth Kinetics, bioRxiv, 2018, p. 456228.
[174] J.W.C. Dunlop, F.D. Fischer, E. Gamsjäger, P. Fratzl, A theoretical model for tissue growth in confined geometries, J. Mech. Phys. Solids 58 (8) (2010) 1073–1087.
[175] M.A. Alias, P.R. Buenzli, Modeling the effect of curvature on the collective behavior of cells growing new tissue, Biophys. J. 112 (1) (2017) 193–204.
[176] M.A. Alias, P.R. Buenzli, Osteoblasts infill irregular pores under curvature and porosity controls: a hypothesis-testing analysis of cell behaviours, Biomechanics Model. Mechanobiol. 17 (5) (2018) 1357–1371.
[177] Y. Guyot, I. Papantoniou, F.P. Luyten, L. Geris, Coupling curvature-dependent and shear stress-stimulated neotissue growth in dynamic bioreactor cultures: a 3D computational model of a complete scaffold, Biomechanics Model. Mechanobiol. 15 (1) (2016) 169–180.
[178] P. Sanaei, L. Cummings, S. Waters, I. Griffiths, Curvature-and fluid-stress-driven tissue growth in a tissue-engineering scaffold pore, Biomechanics Model. Mechanobiol. (2018) 1–17.
[179] A.A. Zadpoor, J. Malda, Additive manufacturing of biomaterials, tissues, and organs, Ann. Biomed. Eng. 45 (1) (2017) 1–11.
[180] F.J. O'Brien, Biomaterials & scaffolds for tissue engineering, Mater. Today 14 (3) (2011) 88–95.
[181] A.A. Zadpoor, Additively manufactured porous metallic biomaterials, J. Mater. Chem. B 7 (2019) 4088–4117.
[182] C. Soyarslan, S. Bargmann, M. Pradas, J. Weissmüller, 3D stochastic bicontinuous microstructures: generation, topology and elasticity, Acta Mater. 149 (2018) 326–340.
[183] A. Vidyasagar, S. Krödel, D. Kochmann, Microstructural patterns with tunable mechanical anisotropy obtained by simulating anisotropic spinodal decomposition, Proc. R. Soc.,A 474 (2218) (2018) 20180535.
[184] F.S.L. Bobbert, K. Lietaert, A.A. Eftekhari, B. Pouran, S.M. Ahmadi, H. Weinans, A.A. Zadpoor, Additively manufactured metallic porous biomaterials based on minimal surfaces: a unique combination of topological, mechanical, and mass transport properties, Acta Biomater. 53 (2017) 572–584.
[185] S.B. Blanquer, M. Werner, M. Hannula, S. Sharifi, G.P. Lajoinie, D. Eglin, J. Hyttinen, A.A. Poot, D.W. Grijpma, Surface curvature in triply-periodic minimal surface architectures as a distinct design parameter in preparing advanced tissue engineering scaffolds, Biofabrication 9 (2) (2017) 025001.
[186] B.M. Willie, A. Petersen, K. Schmidt-Bleek, A. Cipitria, M. Mehta, P. Strube, J. Lienau, B. Wildemann, P. Fratzl, G. Duda, Designing biomimetic scaffolds for bone regeneration: why aim for a copy of mature tissue properties if nature uses a different approach? Soft Matter 6 (20) (2010).
[187] S. Tibbits, 4D printing: multi-material shape change, Architect. Des 84 (1) (2014) 116–121.
[188] T. van Manen, S. Janbaz, A.A. Zadpoor, Programming 2D/3D shape-shifting with hobbyist 3D printers, Mater. Horiz. 4 (6) (2017).
[189] Y. Liu, J.K. Boyles, J. Genzer, M.D. Dickey, Self-folding of polymer sheets using local light absorption, Soft Matter 8 (6) (2012) 1764–1769.
[190] S. Miao, N. Castro, M. Nowicki, L. Xia, H. Cui, X. Zhou, W. Zhu, S. Lee, K. Sarkar, G. Vozzi, Y. Tabata, J. Fisher, L.G. Zhang, 4D printing of polymeric materials for tissue and organ regeneration, Mater. Today 20 (10) (2017) 577–591.
[191] A.S. Gladman, E.A. Matsumoto, R.G. Nuzzo, L. Mahadevan, J.A. Lewis, Biomimetic 4D printing, Nat. Mater. 15 (4) (2016) 413–418.
[192] V.A. Bolaños Quiñones, H. Zhu, A.A. Solovev, Y. Mei, D.H. Gracias, Origami biosystems: 3D assembly methods for biomedical applications, Adv. Biosyst. (2018) 1800230.
[193] T.G. Leong, C.L. Randall, B.R. Benson, N. Bassik, G.M. Stern, D.H. Gracias, Tetherless thermobiochemically actuated microgrippers, Proc. Natl. Acad. Sci. U.S.A. 106 (3) (2009) 703–708.
[194] K. Kuribayashi, K. Tsuchiya, Z. You, D. Tomus, M. Umemoto, T. Ito, M. Sasaki, Self-deployable origami stent grafts as a biomedical application of Ni-rich TiNi shape memory alloy foil, Mater. Sci. Eng., A 419 (1–2) (2006) 131–137.
[195] W. Hu, G.Z. Lum, M. Mastrangeli, M. Sitti, Small-scale soft-bodied robot with multimodal locomotion, Nature 554 (7690) (2018) 81.
[196] S. Miao, W. Zhu, N.J. Castro, M. Nowicki, X. Zhou, H. Cui, J.P. Fisher, L.G. Zhang, 4D printing smart biomedical scaffolds with novel soybean oil epoxidized acrylate, Sci. Rep. 6 (2016) 27226.
[197] R.J. Morrison, S.J. Hollister, M.F. Niedner, M.G. Mahani, A.H. Park, D.K. Mehta, R.G. Ohye, G.E. Green, Mitigation of tracheobronchomalacia with 3D-printed personalized medical devices in pediatric patients, Sci. Transl. Med. 7 (285) (2015) 285ra64-285ra64.
[198] S. Janbaz, N. Noordzij, D.S. Widyaratih, C.W. Hagen, L.E. Fratila-Apachitei, A.A. Zadpoor, Origami lattices with free-form surface ornaments, Sci. Adv. 3 (11) (2017).
[199] S.J. Callens, N. Tümer, A.A. Zadpoor, Hyperbolic origami-inspired folding of triply periodic minimal surface structures, Appl. Mater. Today 15 (2019) 453–461.
[200] C.M. Bidan, M. Fratzl, A. Coullomb, P. Moreau, A.H. Lombard, I. Wang, M. Balland, T. Boudou, N.M. Dempsey, T. Devillers, Magneto-active substrates for local mechanical stimulation of living cells, Sci. Rep. 8 (1) (2018) 1464.
[201] J. Eyckmans, C.S. Chen, Stem cell differentiation: sticky mechanical memory, Nat. Mater. 13 (6) (2014) 542.
[202] C. Yang, M.W. Tibbitt, L. Basta, K.S. Anseth, Mechanical memory and dosing influence stem cell fate, Nat. Mater. 13 (6) (2014) 645.
[203] A.J. Hughes, H. Miyazaki, M.C. Coyle, J. Zhang, M.T. Laurie, D. Chu, Z. Vavrušová, R.A. Schneider, O.D. Klein, Z.J. Gartner, Engineered tissue folding by mechanical compaction of the mesenchyme, Dev. Cell 44 (2) (2018) 165–178. e6.
[204] S. Kaihara, J. Borenstein, R. Koka, S. Lalan, E.R. Ochoa, M. Ravens, H. Pien, B. Cunningham, J.P. Vacanti, Silicon micromachining to tissue engineer branched vascular channels for liver fabrication, Tissue Eng. 6 (2) (2000) 105–117.

[205] G. Vozzi, C. Flaim, A. Ahluwalia, S. Bhatia, Fabrication of PLGA scaffolds using soft lithography and microsyringe deposition, Biomaterials 24 (14) (2003) 2533–2540.
[206] G.M. Whitesides, E. Ostuni, S. Takayama, X. Jiang, D.E. Ingber, Soft lithography in biology and biochemistry, Annu. Rev. Biomed. 3 (1) (2001) 335–373.
[207] T. Weiß, G. Hildebrand, R. Schade, K. Liefeith, Two-photon polymerization for microfabrication of three-dimensional scaffolds for tissue engineering application, Eng. Life Sci. 9 (5) (2009) 384–390.
[208] A. Marino, C. Filippeschi, G.G. Genchi, V. Mattoli, B. Mazzolai, G. Ciofani, The Osteoprint: a bioinspired two-photon polymerized 3-D structure for the enhancement of bone-like cell differentiation, Acta Biomater. 10 (10) (2014) 4304–4313.
[209] A. Khademhosseini, R. Langer, J. Borenstein, J.P. Vacanti, Microscale technologies for tissue engineering and biology, Proc. Natl. Acad. Sci. 103 (8) (2006) 2480–2487.
[210] K. Grosse-Brauckmann, Triply periodic minimal and constant mean curvature surfaces, Interface Focus 2 (5) (2012) 582–588.
[211] Evelyn Spiegel, L. Howard, Lytechinus pictus, embryonic cell, CIL:39782, CIL Dataset, 2012.
[212] O. Bashir, Renal Artery, in: r. 17109 (Ed.) Radiopaedia.org.
[213] A. Puerta, Colonic Diverticulosis: Double Contrast Barium Enema, in: r. 59378 (Ed.) Radiopaedia.org.